

Lectures on the nonlinear stability of the Schwarzschild family of black holes

Martin Taylor*

Spring 2022

Abstract

These notes accompany a 4 lecture mini course on the nonlinear stability of the Schwarzschild family of black holes, given as part of the General Relativity Programme at the Centre of Mathematical Sciences and Applications, Harvard University, from 29th March – 1st April 2022. The lectures concern the following topics:

- Lecture 1: The Schwarzschild and Kerr families, statement of the theorem, boundedness and decay of linear waves on a fixed Schwarzschild background;
- Lecture 2: The Einstein equations in double null gauge and the linear stability of Schwarzschild;
- Lecture 3: The nonlinear stability of Schwarzschild;
- Lecture 4: Conclusions and outlook.

Contents

1	Introduction	2
2	Linear waves on a fixed Schwarzschild exterior	4
2.1	Geometric properties of Schwarzschild	4
2.2	The energy momentum tensor	5
2.3	The Dafermos–Rodnianski r^p method	6
2.4	Linear waves on Minkowski space	7
2.5	Linear waves on a Schwarzschild exterior	9
3	The Einstein equations in double null gauge	13
3.1	Double null gauge	13
3.2	The reduced Einstein equations	16
4	The linear stability of the Schwarzschild family	19
4.1	The linearised equations	20
4.2	Residual pure gauge and linearised Kerr families of solutions	23
4.3	The linear stability theorem	24
4.4	Boundedness and decay for solutions of the Teukolsky equation	25
4.5	Boundedness and decay for the remainder of the linearised system	27

*Imperial College London, Department of Mathematics, South Kensington Campus, London SW7 2AZ, United Kingdom, martin.taylor@imperial.ac.uk.

5	The nonlinear stability of the Schwarzschild family	28
5.1	The null condition and the nonlinear stability of Minkowski space	29
5.2	The nonlinear stability of Schwarzschild theorem	30
5.3	The 3-parameter families of initial data	31
5.4	The logic of the proof	32
5.5	The bootstrap region and the two teleologically normalised gauges	32
5.6	The main estimates	35
5.7	The completion of the continuity argument	37
6	Conclusions and outlook	37
6.1	Properties of \mathcal{I}^+ and \mathcal{H}^+	38
6.2	Axisymmetric solutions with vanishing angular momentum	39
6.3	The nonlinear stability of the Kerr exterior	39
6.4	Extremality and the Aretakis instability	40
6.5	Strong cosmic censorship and the black hole interior	41

1 Introduction

The Schwarzschild family of static black holes,

$$g_M = - \left(1 - \frac{2M}{r}\right) dt^2 + \left(1 - \frac{2M}{r}\right)^{-1} dr^2 + r^2(d\theta^2 + \sin^2 \theta d\phi^2), \quad M > 0, \quad (1.1)$$

constitutes the most famous family of solutions of the vacuum Einstein equations

$$Ric(g) = 0. \quad (1.2)$$

The family was discovered in 1915, shortly after Einstein’s final formulation of (1.2), though it was only understood much later that each member describes a static black hole, and the parameter $M > 0$ has the interpretation of the mass of the black hole as measured by observers at infinity.

More precisely, for each $M > 0$ the local coordinate form (1.1) gives rise to a spherically symmetric, static, asymptotically flat, 3 + 1 dimensional Lorentzian manifold (\mathcal{M}, g_M) which solves (1.2). A complete *future null infinity* \mathcal{I}^+ can be attached to \mathcal{M} , whose causal past is not the entirety of \mathcal{M} , but is bounded to the future by a complete *event horizon* \mathcal{H}^+ at $r = 2M$. Observers can live forever in the black hole exterior region $\{r > 2M\}$.

The most fundamental question one can ask about the Schwarzschild family is whether the exterior of the black hole region is nonlinearly stable as a solution of (1.2). These lectures concern the following theorem, obtained jointly with M. Dafermos, G. Holzegel, and I. Rodnianski [20].

Theorem 1.1 (The full finite co-dimension nonlinear asymptotic stability of Schwarzschild [20]). *The Schwarzschild exterior is nonlinearly asymptotically stable, as a solution of (1.2), to a codimension 3 set of perturbations.*

More precisely, for vacuum initial data sets—with no symmetry assumed—sufficiently close to appropriate Schwarzschild initial data, the resulting maximal Cauchy development

- (i) possesses a complete future null infinity \mathcal{I}^+ whose past $J^-(\mathcal{I}^+)$ is bounded to the future by a regular future complete event horizon \mathcal{H}^+ ,
- (ii) remains globally close to Schwarzschild (1.1) in its exterior,
- (iii) asymptotes back to a member of the Schwarzschild family as a suitable notion of time goes to infinity,

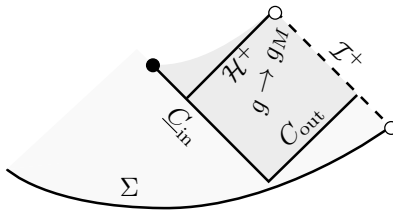


Figure 1: Nonlinear asymptotic stability of Schwarzschild: spacetimes satisfying (i)–(iii).

provided that the initial data set itself lies on a codimension 3 “submanifold” of the moduli space of vacuum initial data. See Section 5.2 for a more precise version of Theorem 1.1.

The codimension 3 restriction is a necessary condition for the asymptotic stability statement (iii). Indeed, as is well known, the Schwarzschild family (1.1) is contained as the $a = 0$ subcase of a larger family of stationary solutions, the Kerr family of uniformly rotating black holes, discovered much later [42], in 1963. In Boyer–Lindquist coordinates the Kerr metric takes the form

$$g_{a,M} = -\frac{\Delta}{\varrho^2}(dt - a \sin^2 \theta d\phi)^2 + \frac{\varrho^2}{\Delta} dr^2 + \varrho^2 d\theta^2 + \frac{\sin^2 \theta}{\varrho^2} (adt - (r^2 + a^2)d\phi)^2, \quad |a| \leq M, \quad M > 0, \quad (1.3)$$

where

$$\Delta = r^2 - 2Mr + a^2, \quad \varrho^2 = r^2 + a^2 \cos^2 \theta.$$

Outside of this codimension 3 submanifold, one expects solutions to necessarily asymptote to a Kerr solution with $a \neq 0$, since the dimension of *linearised Kerr solutions fixing the mass* is equal to 3 in our parametrisation.

The proof of Theorem 1.1 is based on a robust understanding of corresponding linear problems. Indeed, many of the most fundamental aspects of the proof of Theorem 1.1 appear already in the study of the scalar wave equation on a fixed Schwarzschild background, a problem for which much technology has been developed in recent years [7, 24, 6, 26, 25]. See Section 2. The necessary starting point for Theorem 1.1 is a robust understanding of the linear stability of the Schwarzschild family. Such an understanding was first achieved by Dafermos–Holzegel–Rodnianski [19]. See Section 4 for further discussion.

In the absence of symmetry assumptions, the only previous nonlinear stability works on asymptotically flat solutions of (1.2) concern the stability of Minkowski space, first addressed by Christodoulou–Klainerman [15]. Much previous work on nonlinear stability has considered various symmetric reductions, starting from work of Christodoulou on the Einstein–scalar field system in spherical symmetry [11], followed by [23, 16, 36], and most recently, work of Klainerman–Szeftel [47] for polarised axisymmetric spacetimes, which is a first work beyond $1 + 1$ dimensional systems. Note also the work of Hintz–Vasy [35] on the stability of the slowly rotating *Kerr–de Sitter family*, as solutions of the vacuum Einstein equations with a positive cosmological constant $\Lambda > 0$. The reader is referred to [20] for a further discussion of relevant previous works.

The goal of the lectures is to provide a brief description of some of the main steps in the proof of Theorem 1.1. A brief outline is as follows:

- Lecture 1: Boundedness and decay of linear waves on a fixed Schwarzschild background;
- Lecture 2: The Einstein equations in double null gauge and the linear stability of Schwarzschild;
- Lecture 3: The nonlinear stability of Schwarzschild;
- Lecture 4: Conclusions and outlook.

Acknowledgements

I am grateful to M. Dafermos, G. Holzegel, and I. Rodnianski for helpful discussions regarding the preparation of these notes and lectures. I have made extensive use of [20], as well as the lecture notes [26] and [37]. I acknowledge support through Royal Society Tata University Research Fellowship URF\R1\191409.

2 Linear waves on a fixed Schwarzschild exterior

Many of the most fundamental aspects of the proof of Theorem 1.1 arise already in the problem of showing boundedness and decay of solutions of

$$\square_{g_M} \psi = 0, \tag{2.1}$$

arising from smooth localised initial data $\psi|_{\Sigma_0}, \partial_t \psi|_{\Sigma_0}$ (for some appropriate initial hypersurface Σ_0), in the Schwarzschild exterior. Here \square_g denotes the wave operator associated to the Lorentzian metric g ,

$$\square_g \psi = \frac{1}{\sqrt{-\det g}} \partial_\mu (g^{\mu\nu} \sqrt{-\det g} \partial_\nu \psi),$$

which can be appropriately viewed as a ‘‘poor man’s linearisation’’ of Ric around g . The problem of showing boundedness and decay of solutions of (2.1) can thus appropriately be viewed as a poor man’s version of the problem of linear stability of Schwarzschild.

Beyond statements about fixed *mode solutions*, the study of this problem was initiated by Wald [66] in 1979, and has seen an intense level of research over recent years, culminating in the work [27] which addresses this poor man’s linear stability problem for Kerr in the entire subextremal range $|a| < M$.

The discussion here follows [24] and [26]. See [26] for more details and further references.

2.1 Geometric properties of Schwarzschild

Central to the proof of boundedness and decay of solutions of (2.1) is a quantitative understanding of three geometric properties of Schwarzschild:

1. **The redshift effect:** Given a null geodesic $\gamma: (a, b) \rightarrow \mathcal{M}$ and a uniformly timelike vector field $N \in \mathfrak{X}(\mathcal{M})$, one defines the energy of γ with respect to N to be the inner product

$$-g(\dot{\gamma}, N).$$

(Note that, if N is a Killing vector then this energy is conserved along γ .) Taking γ to be an affine parameterisation of one of the null generators of the event horizon of Schwarzschild, written in (t^*, r, θ, ϕ) coordinates defined below in Section 2.5 as

$$\gamma(s) = (t^*(s), r(s), \theta(s), \phi(s)) = (\kappa^{-1} \log s, 2M, \theta_0, \phi_0),$$

where $\kappa = \frac{1}{4M}$ is the *surface gravity* of Schwarzschild, then one sees that the energy with respect to the timelike vector $N = -(dt^*)^\sharp$ satisfies

$$-g(\dot{\gamma}, N) = \frac{1}{\kappa} e^{-\kappa t^*},$$

i.e. the energy of γ is *exponentially decaying*. The ratio

$$\frac{-g(\dot{\gamma}, N)|_{t^*=t_2}}{-g(\dot{\gamma}, N)|_{t^*=t_1}} = e^{-\kappa(t_2-t_1)},$$

has the interpretation of the frequency shift of signals sent by an observer crossing the event horizon at time $t^* = t_1$, as received by an observer crossing the event horizon at the later time $t^* = t_2$. This *exponential redshift* has a damping effect on waves.

2. **Trapped null geodesics:** The null geodesic $\gamma: (-\infty, \infty) \rightarrow \mathcal{M}$ defined in (t, r, θ, ϕ) coordinates by

$$\gamma(s) = (t(s), r(s), \theta(s), \phi(s)) = \left(s, 3M, \frac{\pi}{2}, \frac{s}{\sqrt{27}M} \right),$$

neither escapes to infinity nor crosses the event horizon, but remains trapped at $r = 3M$ for all time. In fact, $\{r = 3M\}$ is spanned by null geodesics and, for any point $p \in \mathcal{M}$ with $r > 2M$, there exists a codimension 1 subset of future directed null vectors whose corresponding null geodesics approach $r = 3M$. Since high frequency waves can localise around null geodesics for long times, the presence of such trapped null geodesics is a potential obstruction to the decay of waves. Any proof of decay of solutions of the wave equation must take advantage of the fact that such trapped null geodesics are *unstable*.

3. **Superradiance** (relevant only in Kerr with $a \neq 0$): The Killing vector field T describing the stationarity of Kerr (the vector field ∂_t in Boyer–Lindquist coordinates (1.3)) is spacelike close to the event horizon, in the *ergoregion*, when $a \neq 0$. There are null geodesics γ whose (conserved) energy with respect to T is *negative*, i.e. $-g(T, \dot{\gamma}) < 0$. In the context of the wave equation, the conserved energy associated to T fails to have a sign close to the event horizon, thus allowing for the existence of waves which travel towards the black hole, divide into a piece with negative energy which falls into the black hole, and a piece with greater positive energy which is reflected. From the point of view of a distant observer, such a wave would be seen to have been sent towards the black hole and then returned with more energy than it began with. A priori, one could also even imagine the existence of waves which are sent towards the black hole with finite energy, and return with *infinite energy*. In showing boundedness and decay of solutions of the wave equation on Kerr with $a \neq 0$, one must quantitatively control how much more energy such a wave can return with (which in particular precludes the existence of the latter type of wave, which returns with infinite energy).

These geometric phenomena are captured and adapted to the study of (2.1) via appropriate *vector field multipliers and commutators*.

2.2 The energy momentum tensor

Given a Lorentzian manifold (\mathcal{M}, g) and a function $\psi: \mathcal{M} \rightarrow \mathbb{R}$, one defines the *energy momentum tensor* $\mathbb{T} = \mathbb{T}[\psi]$ of ψ

$$\mathbb{T}[\psi]_{\mu\nu} = \partial_\mu \psi \partial_\nu \psi - \frac{1}{2} g_{\mu\nu} g^{\alpha\beta} \partial_\alpha \psi \partial_\beta \psi.$$

The energy momentum tensor has the divergence property

$$\nabla^\mu \mathbb{T}[\psi]_{\mu\nu} = \partial_\nu \psi \square_g \psi,$$

and in particular is divergence free if ψ solves the wave equation $\square_g \psi = 0$.

Given a vector field $X \in \mathfrak{X}(\mathcal{M})$, one defines the associated energy current

$$J^X[\psi]_\mu = \mathbb{T}[\psi]_{\mu\nu} X^\nu.$$

Note that

$$\nabla^\mu J^X[\psi]_\mu = X^\nu \square_g \psi + \mathbb{T}[\psi]_{\mu\nu} {}^{(X)}\pi^{\mu\nu}, \tag{2.2}$$

where

$${}^{(X)}\pi_{\mu\nu} = \frac{1}{2} (\mathcal{L}_X g)_{\mu\nu},$$

is the deformation tensor of X . In particular, if X is Killing and $\square_g \psi = 0$, then one obtains the conservation law $\nabla^\mu J^X[\psi]_\mu = 0$. One refers to such a vector field X , when used in (2.2), as a *vector field multiplier*.

Given moreover a function $w: \mathcal{M} \rightarrow \mathbb{R}$, one defines the modified current

$$J^{X,w}[\psi]_\mu = J^X[\psi]_\mu + w\psi\nabla_\mu\psi - \frac{1}{2}\psi^2\nabla_\mu w, \quad (2.3)$$

which satisfies

$$\nabla^\mu J^{X,w}[\psi]_\mu = (X\psi + w\psi)\square_g\psi + \mathbb{T}[\psi]_{\mu\nu}{}^{(X)}\pi^{\mu\nu} + w\nabla^\mu\psi\nabla_\mu\psi - \frac{\psi^2}{2}\square_g w. \quad (2.4)$$

Given a spacetime region $\mathcal{R} \subset \mathcal{M}$, integrating (2.4) over \mathcal{R} leads to the associated energy identity

$$\int_{\mathcal{R}} (X\psi + w\psi)\square_g\psi = \int_{\partial\mathcal{R}} J^{X,w}[\psi]_\mu n_{\partial\mathcal{R}}^\mu - \int_{\mathcal{R}} (\mathbb{T}[\psi]_{\mu\nu}{}^{(X)}\pi^{\mu\nu} + w\nabla^\mu\psi\nabla_\mu\psi - \frac{\psi^2}{2}\square_g w), \quad (2.5)$$

where $n_{\partial\mathcal{R}}$ is an appropriate normal vector to $\partial\mathcal{R}$, and the integrals are taken with respect to appropriate volume forms (note that appropriate orientations have to be chosen on spacelike and null components of $\partial\mathcal{R}$ depending on whether the component lies to the future or past of \mathcal{R} , and there is no *unit* normal or *induced* volume form on the null components . . .). For solutions ψ of the wave equation, $\square_g\psi = 0$, the left hand side of (2.5) of course vanishes.

It is particularly useful to consider timelike multipliers X in regions \mathcal{R} enclosed between spacelike hypersurfaces (whose normal vectors are timelike) in view of the following positivity property.

Proposition 2.1 (Positivity property of \mathbb{T}). *The energy momentum tensor \mathbb{T} has the following positivity property: for any two future directed timelike vector fields $X, Y \in \mathfrak{X}(\mathcal{M})$, the quantity $\mathbb{T}[\psi](X, Y)$ is positive definite in $d\psi$, i.e. in any local coordinate system $\{x^\alpha\}$ there is a constant $C = C(X, Y) > 0$ such that*

$$C^{-1} \sum_{\alpha=0}^3 (\partial_{x^\alpha}\psi)^2 \leq \mathbb{T}[\psi]_{\mu\nu} X^\mu Y^\nu \leq C \sum_{\alpha=0}^3 (\partial_{x^\alpha}\psi)^2.$$

Moreover, if $X, Y \in \mathfrak{X}(\mathcal{M})$ are two causal vectors, then $\mathbb{T}[\psi](X, Y)$ is non-negative definite, i.e.

$$\mathbb{T}[\psi]_{\mu\nu} X^\mu Y^\nu \geq 0.$$

Proof. The proof is left as an exercise. □

2.3 The Dafermos–Rodnianski r^p method

Dafermos–Rodnianski [25] introduced a robust energy based method for showing decay of solutions of wave equations on asymptotically flat spacetimes. The method is modelled on the wave equation

$$\square_m\psi = 0, \quad (2.6)$$

on Minkowski space, (\mathbb{R}^{3+1}, m) , where $m = -dt^2 + (dx^1)^2 + (dx^2)^2 + (dx^3)^2$ is the Minkowski metric, but generalises to a large class of asymptotically flat spacetimes including the Schwarzschild and Kerr exteriors. The approach is particularly well suited to isolating and localising the geometric properties of Schwarzschild described in Section 2.1.

The method applies to stationary spacetimes (\mathcal{M}, g) which are suitably asymptotically flat, to allow for an appropriate hierarchy of r -weighted energy identities in the asymptotically flat region (these r -weighted energy identities arise from applying (2.4) with multiplier $X = r^p\partial_v$, $w = r^{p-1}$ for $0 \leq p \leq 2$ in an appropriate asymptotic region). The method also takes as an input the following ingredients, to be satisfied by all solutions of $\square_g\psi = 0$:

1. Uniform boundedness of a non-degenerate energy:

$$\int_{\Sigma_{t_2}} J_\mu^N[\psi] n_{\Sigma_{t_2}}^\mu \lesssim \int_{\Sigma_{t_1}} J_\mu^N[\psi] n_{\Sigma_{t_1}}^\mu, \quad (2.7)$$

for all $t_2 \geq t_1$, where $\{\Sigma_t\}$ is an appropriate foliation of \mathcal{M} and N is a uniformly timelike vector field (so that the associated energy $J_\mu^N[\psi] n_{\Sigma_t}^\mu$ is non-degenerate — see Proposition 2.1);

2. An integrated local energy decay statement of the form:

$$\int_t^\infty \int_{r \leq R} J_\mu^N[\psi] n^\mu \leq C_R \sum_{k=0}^K \int_{\Sigma_t} J_\mu^N[N^k \psi] n_{\Sigma_t}^\mu, \quad (2.8)$$

for some $K \geq 0$ and all R sufficiently large.

Remark 2.2.

- The estimate (2.7) is manifestly a boundedness statement. The estimate (2.8), on the other hand, should be viewed as a “weak decay” statement for the local energy confined to the compact spatial region $\{r \leq R\}$.
- Note that (2.8) may “lose derivatives” (i.e. more derivatives of ψ may appear on the right hand side than on the left). Some form of such a loss is necessary in Schwarzschild in view of the presence of the trapped null geodesics, described in Section 2.1 (see [64]).

Indeed, the uniform boundedness (2.7) and integrated local energy decay (2.8) statements lead to decay of solutions of $\square_g \psi = 0$. In the case of Minkowski space (2.6), this decay takes the form

$$|r^{\frac{1}{2}} \psi| \lesssim \frac{D}{1 + |t - r|}, \quad |r\psi| \lesssim \frac{D}{1 + |t - r|^{\frac{1}{2}}}, \quad (2.9)$$

where D is an appropriate (higher order, r weighted) initial energy of ψ . The reader is referred to [25] for more details.

Many of the most fundamental aspects of Schwarzschild arise in establishing these two ingredients (2.7) and (2.8) and so, in the interests of time, it is only these two ingredients which will be discussed.

2.4 Linear waves on Minkowski space

First, it is illustrative to discuss (2.7) and (2.8) in the simpler setting of Minkowski space.

Recall that Minkowski space is the manifold \mathbb{R}^{3+1} together with the Minkowski metric m , expressed in Cartesian coordinates as

$$m = -dt^2 + (dx^1)^2 + (dx^2)^2 + (dx^3)^2.$$

In addition to the Cartesian (t, x^1, x^2, x^3) coordinates on \mathbb{R}^{3+1} it is helpful to also consider (t, r, θ, ϕ) , where (r, θ, ϕ) are corresponding polar coordinates on \mathbb{R}^3 , in which the Minkowski metric takes the form

$$m = -dt^2 + dr^2 + r^2(d\theta^2 + \sin^2 \theta d\phi^2).$$

We will consider here (2.7) with hypersurfaces $\Sigma_\tau = \{t = \tau\}$.¹

It is assumed that $\psi: \mathbb{R}^{3+1} \rightarrow \mathbb{R}$ is a smooth solution of

$$\square_m \psi = 0, \quad (2.10)$$

which decays suitably as $r \rightarrow \infty$.

The boundedness statement (2.7) is straightforward to obtain, in view of the fact that Minkowski space admits a uniformly timelike Killing vector field $T = \partial_t$.

Proposition 2.3 (Uniform boundedness of non-degenerate energy for linear waves on Minkowski space). *Let $\psi: \mathbb{R}^{3+1} \rightarrow \mathbb{R}$ solve (2.10). Then ψ satisfies*

$$\int_{\{t=t_2\}} J_\mu^T[\psi] n^\mu \lesssim \int_{\{t=t_1\}} J_\mu^T[\psi] n^\mu, \quad (2.11)$$

¹In fact, the method [25] requires a different foliation, through which the energy *decays*. For example, one could choose Σ_τ to coincide with $\{t = \tau\}$ for $r \leq R$, and with $\{t - r = \tau - R\}$ for $r \geq R$, for some R large, as in [25]. In order to introduce the main ideas in the simplest possible setting, the hypersurfaces $\{t = \tau\}$ are considered here.

or, equivalently,

$$\int_{\{t=t_2\}} ((\partial_t \psi)^2 + |\nabla_x \psi|^2) dx \lesssim \int_{\{t=t_1\}} ((\partial_t \psi)^2 + |\nabla_x \psi|^2) dx,$$

for all $t_2 \geq t_1$ where, in Cartesian coordinates, $T = n = \partial_t$.

Proof. The estimate (2.11) is in fact an *equality*. One sees this easily by noting that

$$J_\mu^T[\psi]n^\mu = \mathbb{T}[\psi]_{tt} = \frac{1}{2}((\partial_t \psi)^2 + |\nabla_x \psi|^2),$$

and differentiating

$$\begin{aligned} \partial_t \left(\int_{\mathbb{R}^3} ((\partial_t \psi)^2 + |\nabla_x \psi|^2)(t, x) dx \right) &= 2 \int_{\mathbb{R}^3} (\partial_t \psi \partial_t^2 \psi + \nabla_x \psi \cdot \nabla_x \partial_t \psi)(t, x) dx \\ &= 2 \int_{\mathbb{R}^3} \partial_t \psi (\partial_t^2 \psi - \Delta_x \psi)(t, x) dx = 0. \end{aligned}$$

A more illuminating version of the proof involves considering (2.4) with $X = T$, $w = 0$, and noting that T is a Killing vector of Minkowski space

$${}^{(T)}\pi = \frac{1}{2} \mathcal{L}_T m = 0.$$

Considering the region $\mathcal{R} = [t_1, t_2] \times \mathbb{R}^3 \subset \mathbb{R}^{3+1}$, the identity (2.5) then implies that

$$\int_{\{t=t_2\}} J_\mu^T[\psi]n^\mu = \int_{\{t=t_1\}} J_\mu^T[\psi]n^\mu.$$

□

The integrated local energy decay statement (2.8) follows from another choice of vector field multiplier.²

Proposition 2.4 (Integrated local energy decay for linear waves on Minkowski space). *Let $\psi: \mathbb{R}^{3+1} \rightarrow \mathbb{R}$ solve (2.10). Then ψ satisfies, for any $\delta > 0$,*

$$\int_t^\infty \int_{\mathbb{R}^3} \left(\frac{1}{r} |\nabla \psi|^2 + \frac{1}{1+r^{1+\delta}} |\partial_t \psi|^2 + \frac{1}{1+r^{1+\delta}} |\partial_r \psi|^2 + \frac{1}{1+r^{3+\delta}} |\psi|^2 \right) (t', x) dx dt' \lesssim \int_{\mathbb{R}^3} J_\mu^T[\psi]n^\mu(t, x) dx, \quad (2.12)$$

for all $t \geq 0$ where, in Cartesian coordinates, $T = n = \partial_t$.

Again, the right hand side of (2.12) can be replaced by

$$\int_{\mathbb{R}^3} ((\partial_t \psi)^2 + |\nabla_x \psi|^2)(t, x) dx.$$

Proof. Consider some $T_1 > t$ and the region $\mathcal{R} = [t, T_1] \times (\mathbb{R}^3 \setminus B(0, \varepsilon))$. The multiplier $X = \partial_r$, $w = \frac{1}{r}$ gives rise to a current (2.3) satisfying

$$\nabla^\mu J_\mu^{X,w} = \frac{1}{r} \left((\partial_t \psi)^2 - (\partial_r \psi)^2 \right) + \frac{1}{r} \nabla^\mu \psi \nabla_\mu \psi = \frac{1}{r} |\nabla \psi|^2.$$

Noting that the boundary terms at times t and T_1 arising in the energy identity (2.5) can be controlled by $J_\mu^T[\psi]n^\mu$ (or, equivalently, by $(\partial_t \psi)^2 + |\nabla_x \psi|^2$), and that the terms on $[t, T_1] \times \partial B(0, \varepsilon)$ vanish in the limit as $\varepsilon \rightarrow 0$, the energy boundedness (2.11) implies that

$$\int_t^{T_1} \int_{\mathbb{R}^3} \frac{1}{r} |\nabla \psi|^2(t', x) dx dt' \lesssim \int_{\mathbb{R}^3} J_\mu^T[\psi]n^\mu(t, x) dx.$$

²The multiplier in fact provides a slightly stronger statement than (2.8), in which the compact set $r \leq R$ is replaced by \mathbb{R}^3 and appropriate decaying weights in r are included (see (2.12)), from which (2.8) trivially follows.

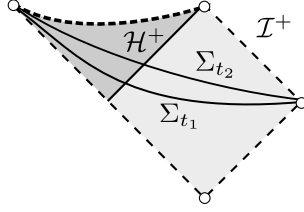


Figure 2: Level hypersurfaces of t^* on a fixed Schwarzschild background.

After letting $T_1 \rightarrow \infty$, this completes the proof for the $\nabla\psi$ term. The remaining terms are controlled similarly by considering (2.3) with $X = \frac{1}{(1+r)^\delta}\partial_r$, $w = \frac{1}{r(1+r)^\delta}$ and noting that

$$\nabla^\mu J_\mu^{X,w} = -\frac{\delta}{2(1+r)^{1+\delta}}(\partial_t\psi)^2 - \frac{\delta}{2(1+r)^{1+\delta}}(\partial_r\psi)^2 - \frac{\delta(1+\delta)}{2r(1+r)^{2+\delta}}\psi^2 + \left(\frac{1}{r(1+r)^\delta} + \frac{\delta}{2(1+r)^{1+\delta}}\right)|\nabla\psi|^2.$$

The details are left as an exercise. \square

2.5 Linear waves on a Schwarzschild exterior

The (t, r, θ, ϕ) coordinate system featuring in the familiar expression (1.1) is often inconvenient in practice, due to its degeneration at $r = 2M$ (note the blow up of the coefficient of dr^2 in (1.1) at $r = 2M$). Accordingly, define

$$t^* = t + 2M \log(r - 2M),$$

and note that, in the resulting (t^*, r, θ, ϕ) coordinate system,

$$g_M = -\left(1 - \frac{2M}{r}\right)(dt^*)^2 + \frac{4M}{r}dt^*dr + \left(1 + \frac{2M}{r}\right)dr^2 + r^2(d\theta^2 + \sin^2\theta d\phi^2), \quad (2.13)$$

Note moreover that $T = \partial_{t^*}$ is a Killing vector field, which is timelike for $r > 2M$, but becomes *null* on the event horizon $r = 2M$. Accordingly, the energy arising from the T multiplier is not coercive but becomes degenerate at $r = 2M$ (and in particular does not give rise to boundedness of a non-degenerate energy of the form (2.7)).

Consider the manifold with corners $\mathcal{M} = [0, \infty) \times [2M, \infty) \times S^2$ equipped with the metric (2.13), and let dV_{S^2} denote the volume form on the unit round sphere. In the standard (θ, ϕ) coordinates

$$dV_{S^2} = \sin\theta d\theta d\phi.$$

It is convenient to consider (2.7) and (2.8) now with hypersurfaces $\Sigma_\tau = \{t^* = \tau\} \times [2M, \infty) \times S^2 \subset \mathcal{M}$ (see Figure 2). Let

$$dV_{\Sigma_\tau} = \left(1 + \frac{2M}{r}\right)^{\frac{1}{2}} r^2 dV_{S^2} dr,$$

denote the volume form on Σ_τ .

It is assumed that $\psi: \mathcal{M} \rightarrow \mathbb{R}$ is a smooth solution of

$$\square_{g_M}\psi = 0, \quad (2.14)$$

which decays suitably as $r \rightarrow \infty$.

Proposition 2.5 (Boundedness of degenerate energy for linear waves on Schwarzschild). *Let $\psi: \mathcal{M} \rightarrow \mathbb{R}$ solve (2.14). Then ψ satisfies*

$$\int_{\Sigma_{t_2}} \left((\partial_{t^*}\psi)^2 + |\nabla\psi|^2 + \left(1 - \frac{2M}{r}\right) (\partial_r\psi)^2 \right) dV_{\Sigma_{t_2}} \lesssim \int_{\Sigma_{t_1}} \left((\partial_{t^*}\psi)^2 + |\nabla\psi|^2 + \left(1 - \frac{2M}{r}\right) (\partial_r\psi)^2 \right) dV_{\Sigma_{t_1}}, \quad (2.15)$$

for all $t_2 \geq t_1 \geq 0$.

Proof. The proof follows from considering (2.4) with $X = T = \partial_{t^*}$, $w = 0$, and recalling that T is a Killing vector

$${}^{(T)}\pi = \frac{1}{2}\mathcal{L}_T g_M = 0.$$

Considering the region $\mathcal{R} = [t_1, t_2] \times [2M, \infty) \times S^2 \subset \mathcal{M}$, the identity (2.5) then implies that

$$\int_{\Sigma_{t_2}} J_\mu^T[\psi]n^\mu + \int_{\mathcal{H}^+(t_1, t_2)} J_\mu^T[\psi]T^\mu = \int_{\Sigma_{t_1}} J_\mu^T[\psi]n^\mu,$$

where n denotes the unit future directed normal to the Σ_t hypersurfaces, and $\mathcal{H}^+(t_1, t_2) = [t_1, t_2] \times \{2M\} \times S^2 \subset \mathcal{H}^+$ denotes the portion of the event horizon between Σ_{t_1} and Σ_{t_2} . The proof then follows from computing $J_\mu^T[\psi]n^\mu$ and noting that

$$\int_{\mathcal{H}^+(t_1, t_2)} J_\mu^T[\psi]T^\mu = \int_{\mathcal{H}^+(t_1, t_2)} (\partial_{t^*}\psi)^2,$$

has a good sign (which can also be inferred from the positivity property, Proposition 2.1). \square

Remark 2.6. Note that (2.15) falls short of (2.7) in view of the degenerate $1 - \frac{2M}{r}$ factor of the $(\partial_r\psi)^2$ term or, equivalently, in view of the fact that the energy density $J_\mu^T[\psi]n^\mu$ is measured with respect to a vector field T which is not uniformly timelike.

Though the estimate (2.15) contains a lot of information (in particular it provides good control over the energy of ψ on $\Sigma_{t_2} \cap \{r \geq 2M + \delta\}$, for all $\delta > 0$), it is entirely consistent with solutions of (or, rather, transverse derivatives of solutions of) $\square_{g_M}\psi = 0$ growing along the event horizon $r = 2M$.³ In order to remove the degeneracy in (2.15) at $r = 2M$, one has to exploit a further property of Schwarzschild. The most convenient way is to capture the redshift property, discussed in Section 2.1, via a multiplier vector field.

Proposition 2.7 (The redshift vector field [26]). *There exists $r_1 > r_0 > 2M$ and a uniformly timelike, future directed vector field N on (\mathcal{M}, g_M) which is t^* invariant (i.e. the Lie derivative along T satisfies $\mathcal{L}_T N = 0$) such that*

$$N = T, \quad \text{for } r \geq r_1,$$

and the associated current satisfies

$$bJ_\mu^N[\psi]N^\mu \leq \nabla^\mu J_\mu^N[\psi], \quad \text{for } 2M \leq r \leq r_0, \quad (2.16)$$

for some constant $b > 0$, for all solutions of $\square_{g_M}\psi = 0$.

The proof is an exercise, or see Section 3 of [26]. The existence of such a vector field does not rely on many properties of Schwarzschild itself. See Section 7 of [26] for a general construction on appropriate black hole spacetimes with positive *surface gravity*.

The vector field N of Proposition 2.7 is called the *redshift* vector field. Note that N is necessarily not Killing (in view of the fact that there are no globally uniformly timelike Killing vector fields on the Schwarzschild exterior), but the property (2.16) means that the additional terms arising in the resulting energy identity have a good sign close to $r = 2M$! The additional terms will not, in general, have a good sign in the region $r_0 \leq r \leq r_1$, but in this region the degenerate energy estimate (2.15) of Proposition 2.5 already provides good control.

³Conservation of such an energy and blow up of such derivatives in fact occurs in extremal black holes. See the discussion of the Aretakis instability in Section 6.4.

Proposition 2.8 (Uniform boundedness of non-degenerate energy for linear waves on Schwarzschild). *Let $\psi: \mathcal{M} \rightarrow \mathbb{R}$ solve (2.14). Then ψ satisfies*

$$\int_{\Sigma_{t_2}} ((\partial_{t^*}\psi)^2 + (\partial_r\psi)^2 + |\nabla\psi|^2) r^2 dV_{\Sigma_{t_2}} \lesssim \int_{\Sigma_{t_1}} ((\partial_{t^*}\psi)^2 + (\partial_r\psi)^2 + |\nabla\psi|^2) r^2 dV_{\Sigma_{t_1}}, \quad (2.17)$$

for all $t_2 \geq t_1 \geq 0$.

Proof. The proof follows from considering (2.4) with $X = N$, $w = 0$, on the region $\mathcal{R} = [t_1, t_2] \times [2M, \infty) \times S^2 \subset \mathcal{M}$, and considering the above sign properties of the resulting bulk term

$$\int_{\mathcal{R}} \mathbb{T}[\psi]_{\mu\nu}^{(N)} \pi^{\mu\nu} = \int_{\mathcal{R}} \nabla^\mu J_\mu^N[\psi],$$

(namely the property (2.16) in $2M \leq r \leq r_0$, the presence of the estimate (2.15) of Proposition 2.5 in the region $r_0 \leq r \leq r_1$, and the fact that $N = T$ and hence $\mathbb{T}[\psi]_{\mu\nu}^{(N)} \pi^{\mu\nu} = \nabla^\mu J_\mu^N[\psi] = 0$ for $r \geq r_1$). The details are left as an exercise, or alternatively see [26]. One in fact moreover has

$$\int_{\mathcal{H}^+(t_1, t_2)} (\partial_{t^*}\psi)^2 + |\nabla\psi|^2 \lesssim \int_{\Sigma_{t_1}} ((\partial_{t^*}\psi)^2 + (\partial_r\psi)^2 + |\nabla\psi|^2) r^2 dV_{\Sigma_{t_1}},$$

where $\mathcal{H}^+(t_1, t_2) = [t_1, t_2] \times \{2M\} \times S^2 \subset \mathcal{H}^+$ denotes the portion of the event horizon between Σ_{t_1} and Σ_{t_2} . \square

Consider now the integrated local energy decay estimate (2.8). Unlike in Minkowski space (see Proposition 2.4), such an integrated local energy decay statement which does not lose derivatives (i.e. a statement of the form (2.8) with $K = 0$) necessarily degenerates at $r = 3M$ in view of the presence of *trapped null geodesics* in the Schwarzschild exterior, discussed in Section 2.1.

Proposition 2.9 (Degenerate integrated local energy decay for linear waves on Schwarzschild). *Let $\psi: \mathcal{M} \rightarrow \mathbb{R}$ solve (2.14). Then ψ satisfies, for any $\delta > 0$,*

$$\int_t^\infty \int_{\Sigma_{t^*}} \frac{1}{r^{3+\delta}} \psi^2 + \frac{1}{r^{1+\delta}} \left(1 - \frac{3M}{r}\right)^2 ((\partial_{t^*}\psi)^2 + (\partial_r\psi)^2 + |\nabla\psi|^2) dV_{\Sigma_{t^*}} dt^* \lesssim \int_{\Sigma_t} J_\mu^N[\psi] n^\mu dV_{\Sigma_t}, \quad (2.18)$$

for all $t \geq 0$.

Remark 2.10. *In addition to (2.18), one moreover has*

$$\int_t^\infty \int_{\Sigma_{t^*}} \frac{1}{r^{1+\delta}} (R\psi)^2 dV_{\Sigma_{t^*}} dt^* \lesssim \int_{\Sigma_t} J_\mu^N[\psi] n^\mu dV_{\Sigma_t},$$

i.e. an integrated local energy decay estimate for the normal derivative

$$R = (dr)^\sharp = \frac{2M}{r} \partial_{t^*} + \left(1 - \frac{2M}{r}\right) \partial_r,$$

to the level hypersurfaces of r , which does not degenerate at $r = 3M$.

Proof of Proposition 2.9. The proof is simpler in (t, r^*, θ, ϕ) coordinates, where

$$r^* = r + 2M \log(r - 2M) - 3M - 2M \log M,$$

in which the Schwarzschild metric takes the form

$$g_M = \left(1 - \frac{2M}{r}\right) (-dt^2 + dr^{*2}) + r^2 (d\theta^2 + \sin^2 \theta d\phi^2).$$

One considers (2.5) with the multiplier

$$X = f(r)\partial_{r^*}, \quad w = \left(1 - \frac{2M}{r}\right)\left(\frac{f'(r)}{2} + \frac{f(r)}{r}\right),$$

and the region $\mathcal{R} = [t^*, T] \times [2M, \infty) \times S^2$, for T large. The divergence (2.4) takes the form

$$\nabla^\mu J^{X,w}[\psi]_\mu = f'(r)(\partial_{r^*}\psi)^2 + \frac{f(r)}{r}\left(1 - \frac{3M}{r}\right)|\nabla\psi|^2 - \frac{1}{2}\psi^2\Box_{g_M}w,$$

and thus, if $f(r)$ is chosen to be a bounded monotonically increasing function, so that $f(r) \sim r - 3M$ near $r = 3M$, $(\Box_{g_M}w)(r = 3M) < 0$, $|\Box_{g_M}w| \lesssim r^{-3-\delta}$, and $|f'(r)| \geq cr^{-1-\delta}$, the estimate (2.5) yields

$$\int_{\mathcal{R}} \left(\frac{1}{r^{1+\delta}}(\partial_{r^*}\psi)^2 + \frac{1}{r}\left(1 - \frac{3M}{r}\right)^2|\nabla\psi|^2 + \chi(r)\psi^2\right) \lesssim \int_{\partial\mathcal{R}} |J^{X,w}[\psi]_\mu n^\mu_{\partial\mathcal{R}}| + \int_{\mathcal{R} \cap \{|r-3M|>\epsilon\}} \frac{1}{r^{3+\delta}}\psi^2,$$

for some small $\epsilon > 0$, where $\chi(r) \geq 0$ is non-vanishing in a neighbourhood of $r = 3M$. If one assumes ψ is supported on spherical harmonics $\ell \geq L$, for some L sufficiently large, then

$$\frac{1}{r^2} \int_{S^2} \psi^2 \leq \frac{1}{L(L+1)} \int_{S^2} |\nabla\psi|^2,$$

and so, if L is sufficiently large, the boundedness estimate of Proposition 2.8 implies that

$$\int_{\mathcal{R}} \left(\frac{1}{r^{1+\delta}}(\partial_{r^*}\psi)^2 + \frac{1}{r}\left(1 - \frac{3M}{r}\right)^2|\nabla\psi|^2 + \frac{1}{r^{3+\delta}}\psi^2\right) \lesssim \int_{\Sigma_t} J_\mu^N[\psi]n^\mu dV_{\Sigma_t}.$$

The remaining $(\partial_t\psi)^2$ term can be estimated by considering (2.5) with

$$X = 0, \quad w = \frac{1}{r^{1+\delta}}\left(1 - \frac{2M}{r}\right)\left(1 - \frac{3M}{r}\right)^2.$$

One then considers a separate multiplier for the $\ell < L$ spherical harmonics. See Section 4.1.1 of [26], or Section 4.1.2 of [26] for an alternative proof which does not rely on a spherical harmonic decomposition. To remove the degeneration at $r = 2M$, one revisits the redshift multiplier of Proposition 2.7. \square

Clearly (2.18) does not constitute an integrated local energy decay estimate of the form (2.8) in view of the degeneration at $r = 3M$. This degeneration can be removed by ‘‘losing a derivative’’. In view of the spherical symmetry of Schwarzschild, there is a basis of Killing vector fields Ω_i , for $i = 1, 2, 3$, spanning the Lie algebra $so(3)$, known as the *angular momentum operators*.

Proposition 2.11 (Non-degenerate integrated local energy decay for linear waves on Schwarzschild). *Let $\psi: \mathcal{M} \rightarrow \mathbb{R}$ solve (2.14). Then ψ satisfies, for any $\delta > 0$,*

$$\int_t^\infty \int_{\Sigma_{t^*}} \frac{1}{r^{1+\delta}}((\partial_{t^*}\psi)^2 + (\partial_r\psi)^2 + |\nabla\psi|^2) dV_{\Sigma_{t^*}} dt^* \lesssim \sum_{k=0}^1 \int_{\Sigma_t} J_\mu^N[N^k\psi]n^\mu dV_{\Sigma_t} + \sum_{i=1}^3 \int_{\Sigma_t} J_\mu^N[\Omega_i\psi]n^\mu dV_{\Sigma_t}, \quad (2.19)$$

for all $t \geq 0$, where $N = \partial_{t^*}$.

Proof. Note the presence of the zeroth order ψ^2 term in (2.18), which does not have a degenerate factor at $r = 3M$. The proof follows by exploiting the good commutation properties of the equation $\Box_{g_M}\psi = 0$ with T and the angular momentum operators Ω_i , for $i = 1, 2, 3$ (namely that if ψ solves (2.14) then so does $T\psi$ and $\Omega_i\psi$). One repeats the above steps for $T\psi$ and $\Omega_i\psi$ and exploits the presence of this zeroth order term. One then revisits the redshift vector field of Proposition 2.7 to remove remaining degeneracy at $r = 2M$. \square

Remark 2.12. Note that, if ψ solves (2.14), then an elliptic estimate implies that

$$\sum_{i=1}^3 \int_{\Sigma_t} J_\mu^N [\Omega_i \psi] n^\mu dV_{\Sigma_t} \lesssim \sum_{k=0}^1 \int_{\Sigma_t} J_\mu^N [N^k \psi] n^\mu dV_{\Sigma_t},$$

and so it is not necessary to include the latter term on the right hand side of (2.19). Such an elliptic estimate can, in fact, be exploited to prove a version of Proposition 2.11 without commuting with $\Omega_1, \Omega_2, \Omega_3$.

The r weights in the boundedness and integrated local energy decay estimates are further improved for certain derivatives via the r^p hierarchy, described in Section 2.3. Moreover, in order to arrive at pointwise decay statements of the form (2.9), analogues of (2.7) and (2.8) for suitable higher order derivatives of ψ are obtained. See [25] and [26] for further details.

Remark 2.13. Though it is the non-degenerate integrated local energy decay estimate of Proposition 2.11 which is used to obtain decay statements of the form (2.9), the existence of the integrated local energy decay estimate of Proposition 2.9, which does not “lose derivatives”, is important for applications to the nonlinear stability problem. The degeneration of this integrated local energy decay estimate complicates the analysis of nonlinear terms close to $r = 3M$. See the discussion in Section 5.6 below.

3 The Einstein equations in double null gauge

Due to the *general covariance* of the vacuum Einstein equations (1.2), one has to *fix a gauge* in order to reduce (1.2) to a well posed system of partial differential equations. The proof [20] of Theorem 1.1 employs a *double null gauge*, intimately related to the Newman–Penrose formalism [57] widely studied in the physics literature, which has a number of desirable features:

- Linear features of double null gauge: *gauge invariant* quantities in the linearisation of (1.2) around Schwarzschild in double null gauge satisfy decoupled *Bardeen–Press* equations, which generalise to Kerr in the form of *Teukolsky* equations. See Section 4.4.
- Nonlinear features of double null gauge: the crucial null structure present in the nonlinearity of (1.2), familiar already from the stability of Minkowski space, is well captured in double null gauge. See Section 5.1 and Section 5.6. Moreover, the event horizon of each solution of Theorem 1.1 is captured as a smooth hypersurface, and the familiar laws of gravitational radiation, along with nonlinear effects such as Christodoulou memory [12], are immediately understood a posteriori. See Section 6.1.

Though the formalism of double null gauge can seem burdensome to the uninitiated, an additional benefit is that the present work can be seen in a unified context with a host of other recent works in general relativity where double null gauge has been successfully employed to describe a wide range of phenomena [14, 46, 45, 53, 52, 21, 18]. In particular, the notation and the form of the equations described below are familiar from these works.

In Section 3.1 a double null gauge of a given spacetime is introduced. In Section 3.2 the Einstein equations are decomposed with respect to double null gauge and recast as a coupled system of elliptic, transport, and hyperbolic equations. The reader is referred to Chapter 1 of [14] for a more detailed discussion.

3.1 Double null gauge

In a given Lorentzian manifold (\mathcal{M}, g) , a double null gauge is a coordinate system u, v, θ^1, θ^2 for \mathcal{M} in which the metric takes the form

$$g = -4\Omega^2 dudv + g_{AB} (d\theta^A - b^A dv)(d\theta^B - b^B dv). \quad (3.1)$$

In such a coordinate system the level hypersurfaces of u and v , denoted C_u and C_v respectively, are null with respect to g , and intersect in spacelike 2-spheres $S_{u,v}$, on which θ^1, θ^2 are coordinates. Here Ω is a

function on \mathcal{M} , b is a vector field on each $S_{u,v}$, and g is the induced metric on $S_{u,v}$, which is assumed to be Riemannian (so that the spheres $S_{u,v}$ are spacelike).

If g takes the double null form (3.1) then the angular coordinates θ^1, θ^2 are moreover constant along the generators of the incoming null hypersurfaces \underline{C}_v . There is an obvious alternative form of (3.1) in which the angular coordinates θ^1, θ^2 are constant along the generators of the outgoing null hypersurfaces C_u .

It is left as an exercise to the reader to show that, if the metric g takes the form (3.1), then the level hypersurfaces of u and v are null.

Note that any Lorentzian metric g on a manifold \mathcal{M} can locally be put in the form (3.1). The Schwarzschild exterior can globally be put in the form (3.1) (modulo the standard degeneration of any coordinate system θ^1, θ^2 on S^2).

Example 3.1 (Schwarzschild in double null gauge). *The Schwarzschild exterior can be written in double null form (3.1) with respect to Eddington–Finkelstein double null coordinates u, v , where the exterior region $r > 2M$ is parameterised by $(-\infty, \infty) \times (-\infty, \infty) \times S^2$. The metric takes the form*

$$g_M = -4 \left(1 - \frac{2M}{r}\right) dudv + r^2 \gamma, \quad (3.2)$$

where $r = r(u, v)$ is determined implicitly by the relation

$$\left(1 - \frac{2M}{r}\right) \frac{r}{2M} \exp\left(\frac{r}{2M}\right) = \exp\left(\frac{v-u}{2M}\right), \quad (3.3)$$

and γ is the unit round metric on S^2 , so that, adding a \circ subscript to denote Schwarzschild quantities,

$$\Omega_\circ^2 = 1 - \frac{2M}{r}, \quad b_\circ = 0, \quad g_\circ = r^2 \gamma.$$

This double null form (3.2) of Schwarzschild can be obtained from the more familiar (1.1) by setting

$$r^* = r + 2M \log(r - 2M) - 3M - 2M \log M, \quad u = \frac{1}{2}(t - r^*), \quad v = \frac{1}{2}(t + r^*).$$

Though the Eddington–Finkelstein double null gauge only parameterises the black hole exterior $r > 2M$, the event horizon \mathcal{H}^+ can be formally parameterised by $\{\infty\} \times (-\infty, \infty) \times S^2$.

See also the Kruskal double null form of Schwarzschild,

$$g_M = -\frac{32M^3}{r} e^{-\frac{r}{2M}} dU dV + r^2 \gamma, \quad (3.4)$$

related to the Eddington–Finkelstein double null u, v by

$$U = -e^{-\frac{u}{2M}}, \quad V = e^{\frac{v}{2M}},$$

which covers the entire maximally extended Schwarzschild manifold. Now the function $r = r(U, V)$ in the expression (3.4) is defined implicitly by the relation

$$\left(1 - \frac{2M}{r}\right) \frac{r}{2M} \exp\left(\frac{r}{2M}\right) = -UV. \quad (3.5)$$

In practice, in the proof of Theorem 1.1, the double null form of Schwarzschild of Example 3.1 is the most convenient representation (despite its degeneration at $r = 2M$).

Note that the Kerr exterior can also be put in the double null form (3.1). See Pretorius–Israel [59].

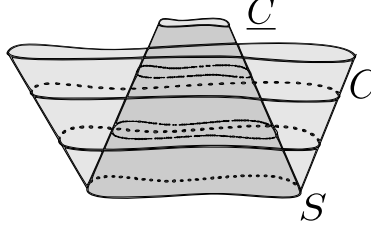


Figure 3: A sphere S in a spacetime (\mathcal{M}, g) and foliations of its corresponding cones C and \underline{C} .

Remark 3.2 (Residual double null freedom). *The condition that the level hypersurfaces of u and v are null, or equivalently that the metric takes the double null form (3.1), does not determine u, v, θ^1, θ^2 completely. In fact, in any given spacetime (\mathcal{M}, g) in which g can be expressed as (3.1), there is an entire infinite dimensional family of diffeomorphisms $\Phi: \mathcal{M} \rightarrow \mathcal{M}$ which preserve the double null form (3.1) of g . The presence of this large degree of residual freedom adds a considerable complication to the proof of Theorem 1.1. See Section 4 (in particular, the discussion in Section 4.5.3) and Section 5.5 below.*

This residual double null freedom can be parameterised as follows. First, one chooses arbitrarily a spacelike 2-sphere S . The boundary of the causal future of S consists of an incoming null cone \underline{C} and an outgoing null cone C . One then chooses speeds at which \underline{C} and C are to be foliated. These speeds then locally induce foliations of \underline{C} and C respectively by spacelike 2-spheres. See Figure 3. The boundaries of the causal futures of these spheres then locally define a spacetime double null foliation. Functions v and u can then be chosen so that their level hypersurfaces coincide with these incoming and outgoing null hypersurfaces respectively, and can be completed to a coordinate system $(u, v, \theta^1, \theta^2)$ by defining coordinates (θ^1, θ^2) on S and extending along the appropriate null generators of these cones. Such a procedure locally defines a double null gauge. Note the infinite dimensional freedom in choosing both S and the speeds at which \underline{C} and C are to be foliated.

Associated to any double null gauge is a *normalised double null frame*

$$e_3 = \frac{1}{\Omega} \partial_u, \quad e_4 = \frac{1}{\Omega} (\partial_v + b^A \partial_{\theta^A}), \quad e_A = \partial_{\theta^A}, \quad A = 1, 2. \quad (3.6)$$

The frame is normalised so that

$$g(e_3, e_4) = -2, \quad g(e_3, e_3) = g(e_3, e_4) = g(e_3, e_A) = g(e_4, e_A) = 0, \quad A = 1, 2.$$

The Ricci coefficients of this double null frame are denoted

$$\chi_{AB} := g(\nabla_{e_A} e_4, e_B), \quad \underline{\chi}_{AB} := g(\nabla_{e_A} e_3, e_B), \quad (3.7)$$

$$\eta_A := -\frac{1}{2} g(\nabla_{e_3} e_A, e_4), \quad \underline{\eta}_A := -\frac{1}{2} g(\nabla_{e_4} e_A, e_3), \quad (3.8)$$

$$\hat{\omega} := \frac{1}{2} g(\nabla_{e_4} e_3, e_4), \quad \underline{\hat{\omega}} := \frac{1}{2} g(\nabla_{e_3} e_4, e_3), \quad (3.9)$$

with χ and $\underline{\chi}$ further decomposed into their trace and trace free parts as

$$\text{tr}\chi := g^{AB} \chi_{AB}, \quad \text{tr}\underline{\chi} := g^{AB} \underline{\chi}_{AB}, \quad \hat{\chi}_{AB} := \chi_{AB} - \frac{1}{2} \text{tr}\chi g_{AB}, \quad \underline{\hat{\chi}}_{AB} := \underline{\chi}_{AB} - \frac{1}{2} \text{tr}\underline{\chi} g_{AB},$$

and the curvature components are denoted

$$\alpha_{AB} := R(e_A, e_4, e_B, e_4), \quad \underline{\alpha}_{AB} := R(e_A, e_3, e_B, e_3), \quad (3.10)$$

$$\beta_A := \frac{1}{2} R(e_A, e_4, e_3, e_4), \quad \underline{\beta}_A := \frac{1}{2} R(e_A, e_3, e_3, e_4), \quad (3.11)$$

$$\rho := \frac{1}{4} R(e_4, e_3, e_4, e_3), \quad \sigma := \frac{1}{4} R(e_4, e_3, e_4, e_3). \quad (3.12)$$

Here, R denotes the Riemann curvature tensor of g , defined as usual by

$$R(W, Z, X, Y) = g(R(X, Y)Z, W) = g(\nabla_X \nabla_Y Z - \nabla_Y \nabla_X Z - [X, Y]Z, W)$$

and $*$ denotes the Hodge star operation. Note that $\text{tr}\chi$, $\text{tr}\underline{\chi}$, $\hat{\omega}$, $\hat{\omega}$, ρ , σ are spacetime functions, η , $\underline{\eta}$, β , $\underline{\beta}$ are one forms on the spheres $S_{u,v}$, and $\hat{\chi}$, $\underline{\hat{\chi}}$, α , $\underline{\alpha}$ are symmetric trace free $(0, 2)$ tensor fields on the spheres $S_{u,v}$.

Example 3.3 (Geometric quantities of Schwarzschild in double null gauge). *In the Eddington–Finkelstein double null gauge of Schwarzschild, described in Example 3.1, along with the metric quantities*

$$\Omega_\circ^2 = 1 - \frac{2M}{r}, \quad b_\circ = 0, \quad \not\partial_\circ = r^2 \gamma, \quad (3.13)$$

the non-vanishing Ricci coefficients take the form

$$(\Omega \text{tr}\chi)_\circ = \frac{2}{r} \left(1 - \frac{2M}{r}\right), \quad (\Omega \text{tr}\underline{\chi})_\circ = -\frac{2}{r} \left(1 - \frac{2M}{r}\right), \quad (\Omega \hat{\omega})_\circ = \frac{M}{r^2}, \quad (\Omega \hat{\omega})_\circ = -\frac{M}{r^2}, \quad (3.14)$$

and the only non-vanishing curvature component takes the form

$$\rho_\circ = -\frac{2M}{r^3}. \quad (3.15)$$

3.2 The reduced Einstein equations

In order to geometrically capture the analytic content of the vacuum Einstein equations, in double null gauge the Ricci coefficients and curvature components, described in Section 3.1, are considered as the unknowns. The reduced Einstein equations consist of the null components of the *structure equations*, satisfied by the Ricci coefficients, and the null *Bianchi equations* satisfied by the curvature components.

Consider a spacetime (\mathcal{M}, g) together with a double null gauge, as described in Section 3.1. Let ξ denote a $(0, k)$ $S_{u,v}$ -tensor field, i.e. a $(0, k)$ tensor field on \mathcal{M} such that

$$\xi(X_1, \dots, X_k) = 0,$$

whenever $X_i \in \{e_3, e_4\}$ for some $i = 1, \dots, k$. One defines $\nabla_3 \xi$ and $\nabla_4 \xi$ to be the restriction of $\nabla_{e_3} \xi$ and $\nabla_{e_4} \xi$ respectively to $S_{u,v}$ tangent vectors $V_1, \dots, V_k \in T_p S_{u,v}$. One moreover defines ∇ to be the Levi-Civita connection of the spheres $(S_{u,v}, \not\partial)$.

The null components of the relations

$$\nabla_X Y - \nabla_Y X = [X, Y], \quad [\nabla_X, \nabla_Y]Z - \nabla_{[X, Y]}Z = R(X, Y)Z, \quad (3.16)$$

together with the vacuum Einstein equations (1.2), provide relations between the null Ricci coefficients (3.7)–(3.9) and the null curvature components (3.10)–(3.12). Examples are

$$\nabla_4 \hat{\chi} + \text{tr}\chi \hat{\chi} - \hat{\omega} \hat{\chi} = -\alpha, \quad \text{d}\not\chi \hat{\chi} = \frac{1}{2} \hat{\chi}^\sharp \cdot (\eta - \underline{\eta}) - \frac{1}{2} \text{tr}\underline{\chi} \eta + \frac{1}{2\Omega} \nabla (\Omega \text{tr}\underline{\chi}) + \underline{\beta}. \quad (3.17)$$

The former of (3.17) can be viewed as a *transport* equation for $\hat{\chi}$, while the latter can be viewed as an *elliptic* equation for $\hat{\chi}$ on the spheres $S_{u,v}$.

Recall that, in any Lorentzian manifold (\mathcal{M}, g) , the second Bianchi identity leads to the relation

$$\nabla^\alpha R_{\alpha\beta\gamma\delta} = \nabla_\gamma \text{Ric}_{\beta\delta} - \nabla_\delta \text{Ric}_{\beta\gamma}.$$

It follows that, for any solution of (1.2), the Riemann curvature tensor is divergence free

$$\nabla^\alpha R_{\alpha\beta\gamma\delta} = 0. \quad (3.18)$$

The null components of (3.18) lead to a further set of relations between the null curvature components (3.10)–(3.12) and the null Ricci coefficients (3.7)–(3.9). Examples are

$$\nabla_3 \alpha + \frac{1}{2} \text{tr} \chi \alpha + 2 \hat{\omega} \alpha = -2 \mathcal{D}_2^* \beta - 3 \hat{\chi} \rho - 3^* \hat{\chi} \sigma + \frac{1}{2} (9\eta - \underline{\eta}) \hat{\otimes} \beta, \quad \nabla_4 \beta + 2 \text{tr} \chi \beta - \hat{\omega} \beta = \text{d}\not{v} \alpha + \eta^\sharp \cdot \alpha. \quad (3.19)$$

Here $-2\mathcal{D}_2^*$ and $\text{d}\not{v}$ denote the symmetric trace free gradient and divergence with respect to \not{g} respectively, defined below in (3.22) and (3.20) respectively. This system of *Bianchi equations* is to be viewed as a *hyperbolic* system for the null curvature components.

Remark 3.4 (Hyperbolicity of the Bianchi equations). *Indeed, considering the examples (3.19), one notes that, for any $S_{u,v}$ one form ξ and any $S_{u,v}$ trace free (0,2) tensor ϑ ,*

$$\int_{S_{u,v}} (\xi, \text{d}\not{v} \vartheta)_{\not{g}} = \int_{S_{u,v}} (\mathcal{D}_2^* \xi, \vartheta)_{\not{g}},$$

i.e. \mathcal{D}_2^ is the formal $L^2(S_{u,v}, \not{g})$ adjoint of $\text{d}\not{v}$. This fact leads to an energy estimate for the pair (α, β) . Indeed, for simplicity suppose α and β are $S_{u,v}$ tensors on a fixed Minkowski background (on which $e_3 = \partial_u$, $e_4 = \partial_v$). If*

$$\nabla_3 \alpha = -2 \mathcal{D}_2^* \beta + \dots, \quad \nabla_4 \beta = \text{d}\not{v} \alpha + \dots,$$

then

$$\frac{1}{2} \partial_u (|\alpha|^2) + \partial_v (|\beta|^2) = \alpha \cdot \nabla_3 \alpha + 2\beta \cdot \nabla_4 \beta = -2\alpha \cdot \mathcal{D}_2^* \beta + 2\beta \cdot \text{d}\not{v} \alpha + \dots = 2 \text{d}\not{v} (\alpha \cdot \beta) + \dots$$

Integrating over a spacetime region of the form $[u_1, u_2] \times [v_1, v_2] \times S^2$, for some $u_2 > u_1$, $v_2 > v_1$ then yields an energy identity

$$\frac{1}{2} \int_{u=u_2} |\alpha|^2 + \int_{v=v_2} |\beta|^2 = \frac{1}{2} \int_{u=u_1} |\alpha|^2 + \int_{v=v_1} |\beta|^2 + \dots$$

The full list of null structure and Bianchi equations is stated here for convenience.

For totally symmetric covariant $S_{u,v}$ -tensors ϕ of rank $s+1$, define the covariant rank s $S_{u,v}$ -tensors

$$(\text{d}\not{v} \phi)_{A_1 \dots A_s} := \not{g}^{BC} \nabla_B \phi_{CA_1 \dots A_s} \quad (3.20)$$

$$(\text{curl} \phi)_{A_1 \dots A_s} := \not{e}^{BC} \nabla_B \phi_{CA_1 \dots A_s}. \quad (3.21)$$

For $S_{u,v}$ -tangent 1-forms ξ define the operator

$$\mathcal{D}_2^* \xi = -\frac{1}{2} \left(\nabla \xi + \nabla^T \xi - \text{d}\not{v} \xi \not{g} \right), \quad (3.22)$$

where $\nabla^T \xi$ denotes the transpose of $\nabla \xi$,

$$(\nabla^T \xi)_{AB} = \nabla_B \xi_A. \quad (3.23)$$

In addition to the above differential operators, define the following algebraic operations on $S_{u,v}$ -tensors. Let ϑ_{AB} and $\tilde{\vartheta}_{AB}$ be symmetric covariant $S_{u,v}$ -tangent (0,2)-tensors and $\xi_A, \tilde{\xi}_A$ be covariant $S_{u,v}$ -tangent 1-forms. Define

$$\begin{aligned} (\vartheta \times \tilde{\vartheta})_{BC} &:= \not{g}^{AD} \vartheta_{AB} \tilde{\vartheta}_{DC} \\ (\vartheta, \tilde{\vartheta}) &:= \not{g}^{AC} \not{g}^{BD} \vartheta_{AB} \tilde{\vartheta}_{CD} \\ (\xi, \tilde{\xi}) &:= \not{g}^{AB} \xi_A \tilde{\xi}_B \\ (\xi \hat{\otimes} \tilde{\xi})_{AB} &:= \xi_A \tilde{\xi}_B + \xi_B \tilde{\xi}_A - \not{g}^{CD} \xi_C \tilde{\xi}_D \not{g}_{AB} \\ \vartheta \wedge \tilde{\vartheta} &:= \not{e}^{AB} \not{g}^{CD} \vartheta_{AC} \tilde{\vartheta}_{BD}. \end{aligned}$$

For totally symmetric covariant $S_{u,v}$ -tensors of rank $s + 2$ define

$$(\text{tr}\phi)_{A_1\dots A_s} := \not{g}^{BC} \phi_{BCA_1\dots A_s}.$$

For $S_{u,v}$ -tangent 1-forms ξ_A and symmetric covariant $S_{u,v}$ -tangent 2-tensors ϑ_{AB} define the Hodge duals ${}^*\xi_A$ and ${}^*\vartheta_{AB}$ by the expressions

$${}^*\xi_A := \not{g}_{AC} \not{e}^{CB} \xi_B, \quad {}^*\vartheta_{AB} := \not{g}_{BD} \not{e}^{DC} \vartheta_{AC}.$$

For a (not necessarily symmetric) 2-covariant $S_{u,v}$ -tensor field ϑ_{AB} and an $S_{u,v}$ -tangent 1-form ξ_A , recall the musical isomorphisms

$$\vartheta_A^\#{}^C = \vartheta_{AB} \not{g}^{BC}, \quad \xi^\#{}^C = \xi_A \not{g}^{AC},$$

defining $S_{u,v}$ -tangent (1, 1) and (1, 0) tensors, respectively.

For a $(0, k)$ $S_{u,v}$ -tensor T , consider also the coercive expression

$$|T|_{\not{g}}^2 := \not{g}^{A_1 B_1} \dots \not{g}^{A_k B_k} T_{A_1\dots A_k} T_{B_1\dots B_k}. \quad (3.24)$$

Proposition 3.5 (Null structure and Bianchi equations). *The null structure equations (3.16) in full take the form*

$$\nabla_3 \underline{\hat{\chi}} + \text{tr}\underline{\chi} \underline{\hat{\chi}} - \underline{\hat{\omega}} \underline{\hat{\chi}} = -\underline{\alpha}, \quad \nabla_4 \underline{\hat{\chi}} + \text{tr}\underline{\chi} \underline{\hat{\chi}} - \underline{\hat{\omega}} \underline{\hat{\chi}} = -\underline{\alpha}, \quad (3.25)$$

$$\nabla_3 \text{tr}\underline{\chi} + \frac{1}{2} (\text{tr}\underline{\chi})^2 - \underline{\hat{\omega}} \text{tr}\underline{\chi} = -(\underline{\hat{\chi}}, \underline{\hat{\chi}}), \quad \nabla_4 \text{tr}\underline{\chi} + \frac{1}{2} (\text{tr}\underline{\chi})^2 - \underline{\hat{\omega}} \text{tr}\underline{\chi} = -(\underline{\hat{\chi}}, \underline{\hat{\chi}}). \quad (3.26)$$

$$\nabla_3 \underline{\hat{\chi}} + \frac{1}{2} \text{tr}\underline{\chi} \underline{\hat{\chi}} + \underline{\hat{\omega}} \underline{\hat{\chi}} = -2\underline{\mathcal{D}}_2^* \underline{\eta} - \frac{1}{2} \text{tr}\underline{\chi} \underline{\hat{\chi}} + \underline{\eta} \widehat{\otimes} \underline{\eta}, \quad (3.27)$$

$$\nabla_4 \underline{\hat{\chi}} + \frac{1}{2} \text{tr}\underline{\chi} \underline{\hat{\chi}} + \underline{\hat{\omega}} \underline{\hat{\chi}} = -2\underline{\mathcal{D}}_2^* \underline{\eta} - \frac{1}{2} \text{tr}\underline{\chi} \underline{\hat{\chi}} + \underline{\eta} \widehat{\otimes} \underline{\eta}, \quad (3.28)$$

$$\nabla_3 \text{tr}\underline{\chi} + \frac{1}{2} \text{tr}\underline{\chi} \text{tr}\underline{\chi} + \underline{\hat{\omega}} \text{tr}\underline{\chi} = -(\underline{\hat{\chi}}, \underline{\hat{\chi}}) + 2(\underline{\eta}, \underline{\eta}) + 2\rho + 2\text{d}\not{I}v\underline{\eta}, \quad (3.29)$$

$$\nabla_4 \text{tr}\underline{\chi} + \frac{1}{2} \text{tr}\underline{\chi} \text{tr}\underline{\chi} + \underline{\hat{\omega}} \text{tr}\underline{\chi} = -(\underline{\hat{\chi}}, \underline{\hat{\chi}}) + 2(\underline{\eta}, \underline{\eta}) + 2\rho + 2\text{d}\not{I}v\underline{\eta}, \quad (3.30)$$

$$\nabla_3 \underline{\eta} + \frac{1}{2} \text{tr}\underline{\chi} \underline{\eta} = \frac{1}{2} \text{tr}\underline{\chi} \underline{\eta} + \underline{\hat{\chi}}^\# \cdot (\underline{\eta} - \underline{\eta}) + \underline{\beta}, \quad \nabla_4 \underline{\eta} + \frac{1}{2} \text{tr}\underline{\chi} \underline{\eta} = \frac{1}{2} \text{tr}\underline{\chi} \underline{\eta} - \underline{\hat{\chi}}^\# \cdot (\underline{\eta} - \underline{\eta}) - \underline{\beta}, \quad (3.31)$$

$$\nabla_4 \underline{\eta} + \text{tr}\underline{\chi} \underline{\eta} = \frac{2}{\Omega} \nabla(\Omega \underline{\hat{\omega}}) + \underline{\beta} - 2\underline{\hat{\chi}} \cdot \underline{\eta}, \quad (3.32)$$

$$\nabla_3 \underline{\eta} + \text{tr}\underline{\chi} \underline{\eta} = \frac{2}{\Omega} \nabla(\Omega \underline{\hat{\omega}}) - \underline{\beta} - 2\underline{\hat{\chi}} \cdot \underline{\eta}, \quad (3.33)$$

$$\Omega^{-1} \nabla_4(\Omega \underline{\hat{\omega}}) = 2(\underline{\eta}, \underline{\eta}) - |\underline{\eta}|^2 - \rho, \quad \Omega^{-1} \nabla_3(\Omega \underline{\hat{\omega}}) = 2(\underline{\eta}, \underline{\eta}) - |\underline{\eta}|^2 - \rho, \quad (3.34)$$

$$\text{curl}\underline{\eta} = -\frac{1}{2} \underline{\hat{\chi}} \wedge \underline{\hat{\chi}} + \underline{\sigma}, \quad \text{curl}\underline{\eta} = \frac{1}{2} \underline{\hat{\chi}} \wedge \underline{\hat{\chi}} - \underline{\sigma}, \quad (3.35)$$

$$d\dot{v}\hat{\chi} = -\frac{1}{2}\hat{\chi}^\sharp \cdot (\eta - \underline{\eta}) - \frac{1}{2}\text{tr}\chi\underline{\eta} + \frac{1}{2\Omega}\nabla(\Omega\text{tr}\chi) - \beta, \quad (3.36)$$

$$d\dot{v}\hat{\underline{\chi}} = \frac{1}{2}\hat{\underline{\chi}}^\sharp \cdot (\eta - \underline{\eta}) - \frac{1}{2}\text{tr}\underline{\chi}\eta + \frac{1}{2\Omega}\nabla(\Omega\text{tr}\underline{\chi}) + \underline{\beta}, \quad (3.37)$$

$$K = -\frac{1}{4}\text{tr}\chi\text{tr}\underline{\chi} + \frac{1}{2}(\hat{\chi}, \hat{\underline{\chi}}) - \rho, \quad (3.38)$$

where K denotes the Gauss curvature of $(S_{u,v}, \mathfrak{g})$, the Bianchi equations (3.18) take the form

$$\nabla_3\alpha + \frac{1}{2}\text{tr}\chi\alpha + 2\hat{\omega}\alpha = -2\mathcal{D}_2^*\beta - 3\hat{\chi}\rho - 3^*\hat{\chi}\sigma + \frac{1}{2}(9\underline{\eta} - \underline{\eta}) \hat{\otimes}\beta, \quad (3.39)$$

$$\nabla_4\beta + 2\text{tr}\chi\beta - \hat{\omega}\beta = d\dot{v}\alpha + \eta^\sharp \cdot \alpha, \quad (3.40)$$

$$\nabla_3\beta + \text{tr}\chi\beta + \hat{\omega}\beta = \nabla\rho + {}^*\nabla\sigma + 3\underline{\eta}\rho + 3^*\underline{\eta}\sigma + 2\hat{\chi}^\sharp \cdot \beta, \quad (3.41)$$

$$\nabla_4\rho + \frac{3}{2}\text{tr}\chi\rho = d\dot{v}\beta + \frac{1}{2}(\eta + 3\underline{\eta}, \beta) - \frac{1}{2}(\hat{\underline{\chi}}, \alpha), \quad (3.42)$$

$$\nabla_4\sigma + \frac{3}{2}\text{tr}\chi\sigma = -\text{curl}\beta - \frac{1}{2}(\eta + 3\underline{\eta}) \wedge \beta + \frac{1}{2}\hat{\underline{\chi}} \wedge \alpha, \quad (3.43)$$

$$\nabla_3\rho + \frac{3}{2}\text{tr}\chi\rho = -d\dot{v}\underline{\beta} - \frac{1}{2}(3\underline{\eta} + \underline{\eta}, \underline{\beta}) - \frac{1}{2}(\hat{\underline{\chi}}, \underline{\alpha}), \quad (3.44)$$

$$\nabla_3\sigma + \frac{3}{2}\text{tr}\chi\sigma = -\text{curl}\underline{\beta} - \frac{1}{2}(3\underline{\eta} + \underline{\eta}) \wedge \underline{\beta} - \frac{1}{2}\hat{\underline{\chi}} \wedge \underline{\alpha}, \quad (3.45)$$

$$\nabla_4\underline{\beta} + \text{tr}\chi\underline{\beta} + \hat{\omega}\underline{\beta} = -\nabla\rho + {}^*\nabla\sigma - 3\underline{\eta}\rho + 3^*\underline{\eta}\sigma + 2\hat{\underline{\chi}}^\sharp \cdot \beta, \quad (3.46)$$

$$\nabla_3\underline{\beta} + 2\text{tr}\chi\underline{\beta} - \hat{\omega}\underline{\beta} = -d\dot{v}\alpha - \eta^\sharp \cdot \alpha, \quad (3.47)$$

$$\nabla_4\underline{\alpha} + \frac{1}{2}\text{tr}\chi\underline{\alpha} + 2\hat{\omega}\underline{\alpha} = 2\mathcal{D}_2^*\underline{\beta} - 3\hat{\underline{\chi}}\rho + 3^*\hat{\underline{\chi}}\sigma - \frac{1}{2}(9\underline{\eta} - \underline{\eta}) \hat{\otimes}\underline{\beta}. \quad (3.48)$$

and one moreover has the following equations satisfied by the metric components

$$\nabla_3\mathfrak{g} = \nabla_4\mathfrak{g} = 0, \quad (3.49)$$

$$\partial_u b^A = 2\Omega^2(\eta^A - \underline{\eta}^A), \quad (3.50)$$

$$\eta + \underline{\eta} = 2\nabla\log\Omega, \quad \hat{\omega} = \nabla_4\log\Omega, \quad \hat{\omega} = \nabla_3\log\Omega. \quad (3.51)$$

Proof. The proof is left as an exercise. Alternatively, see Chapter 1 of [14] for a detailed derivation. \square

Equations (3.26) are known as the *Raychaudhuri equations*. Equations (3.36) and (3.37) constitute the *Codazzi equations*, and equation (3.38) the *Gauss equation*.

A solution $\text{tr}\chi$, $\text{tr}\underline{\chi}$, $\hat{\chi}$, $\hat{\underline{\chi}}$, $\hat{\omega}$, $\hat{\omega}$, η , $\underline{\eta}$, α , $\underline{\alpha}$, β , $\underline{\beta}$, ρ , σ , Ω , b , \mathfrak{g} of (3.25)–(3.51) moreover gives rise to a solution of the vacuum Einstein equations (1.2) in double null gauge. In the remainder, it is this reduced system (3.25)–(3.51) (or its linearisation around Schwarzschild) which is studied.

4 The linear stability of the Schwarzschild family

In this section the problem of the *linear stability* of the Schwarzschild family in double null gauge is discussed. The problem concerns boundedness and decay properties of the reduced Einstein equations in double null gauge (3.25)–(3.51) linearised around the Schwarzschild solution (or more precisely the Schwarzschild solution in the Eddington–Finkelstein double null gauge described in Example 3.3). The first full resolution of this problem is due to Dafermos–Holzegel–Rodnianski [19].

Theorem 4.1 (Dafermos–Holzegel–Rodnianski [19]). *The Schwarzschild exterior is linearly stable as a solution of the vacuum Einstein equations (1.2).*

See Section 4.3 below for a more precise formulation of the linear stability theorem.

A version of Theorem 4.1 has also, more recently, been shown in a *generalised harmonic gauge* [41]. See also [38, 39] and, for some results on Kerr, see [1, 34].

This full linear stability problem contains all of the difficulties of the poor man’s linear stability problem, described in Section 2, and is further complicated by the following facts:

- A decoupled wave equation, which can be analysed using the methods described in Section 2, does not directly emerge from the linearisation of the reduced equations (3.25)–(3.51). See Section 4.4 for a discussion of the decoupled Teukolsky equation, and the Chandrasekhar transformations employed in [19] to arrive at such a wave equation which can be studied using the insights described in Section 2.
- The linearised equations admit families of non-decaying solutions. The existence of such solutions can be inferred in view of the presence of other nearby members of the Kerr family (1.3), and the infinite dimensional residual double null freedom described in Remark 3.2. See Section 4.2 below for a further description of these non-decaying solutions of the linearised equations.

In Section 4.1 the linearised vacuum Einstein equations in double null gauge around the Schwarzschild are discussed. In Section 4.2 the two families of non-decaying solutions are introduced. In Section 4.3 the linear stability theorem, Theorem 4.1, is stated more precisely, and in Sections 4.4 and 4.5 the proof is discussed.

4.1 The linearised equations

The system (3.25)–(3.51) of reduced Einstein equations in double null gauge is formally linearised around the Schwarzschild solution in Eddington–Finkelstein double null gauge (3.13)–(3.15) as follows. One considers the Eddington–Finkelstein double null parameterisation of the Schwarzschild exterior $\mathcal{M} = (-\infty, \infty) \times (-\infty, \infty) \times S^2$ (see Example 3.1), and a one parameter family of metrics in double null form

$$g(\varepsilon) = -4\Omega^2(\varepsilon)dudv + \not{g}_{AB}(\varepsilon)(d\theta^A - b^A(\varepsilon)dv)(d\theta^B - b^B(\varepsilon)dv),$$

on this background, such that $g(0)$ is the Schwarzschild metric in Eddington–Finkelstein double null form

$$g(0) = -4 \left(1 - \frac{2M}{r} \right) dudv + r^2 \gamma.$$

One considers the associated Ricci coefficients and curvature components (3.7)–(3.12) and formally Taylor expands around the corresponding Schwarzschild quantities

$$\begin{aligned} \Omega(\varepsilon) &= \Omega_{\circ} + \varepsilon \overset{(\circ)}{\Omega} + \mathcal{O}(\varepsilon^2), \\ \not{g}(\varepsilon) &= \not{g}_{\circ} + \varepsilon \overset{(\circ)}{\not{g}} + \mathcal{O}(\varepsilon^2), \\ \Omega \text{tr} \chi(\varepsilon) &= \Omega \text{tr} \chi_{\circ} + \varepsilon (\Omega \text{tr} \chi)_{\circ} + \mathcal{O}(\varepsilon^2), \\ \Omega \text{tr} \underline{\chi}(\varepsilon) &= \Omega \text{tr} \underline{\chi}_{\circ} + \varepsilon (\Omega \text{tr} \underline{\chi})_{\circ} + \mathcal{O}(\varepsilon^2), \\ \Omega \hat{\omega}(\varepsilon) &= \Omega \hat{\omega}_{\circ} + \varepsilon \overset{(\circ)}{\hat{\omega}} + \mathcal{O}(\varepsilon^2), \\ \Omega \hat{\omega}(\varepsilon) &= \Omega \hat{\omega}_{\circ} + \varepsilon \overset{(\circ)}{\hat{\omega}} + \mathcal{O}(\varepsilon^2), \\ \rho(\varepsilon) &= \rho_{\circ} + \varepsilon \overset{(\circ)}{\rho} + \mathcal{O}(\varepsilon^2), \end{aligned}$$

for appropriate $\overset{(\circ)}{\Omega}$, $\overset{(\circ)}{\not{g}}$, etc., where the \circ subscript denotes the Schwarzschild quantities of Example 3.3, along with the quantities which vanish in Schwarzschild in Eddington–Finkelstein gauge

$$b(\varepsilon) = \varepsilon \overset{(\circ)}{b} + \mathcal{O}(\varepsilon^2), \quad \hat{\chi}(\varepsilon) = \varepsilon \overset{(\circ)}{\hat{\chi}} + \mathcal{O}(\varepsilon^2), \quad \underline{\hat{\chi}}(\varepsilon) = \varepsilon \overset{(\circ)}{\underline{\hat{\chi}}} + \mathcal{O}(\varepsilon^2), \quad \eta(\varepsilon) = \varepsilon \overset{(\circ)}{\eta} + \mathcal{O}(\varepsilon^2), \quad \underline{\eta}(\varepsilon) = \varepsilon \overset{(\circ)}{\underline{\eta}} + \mathcal{O}(\varepsilon^2),$$

and

$$\alpha(\varepsilon) = \varepsilon \overset{(1)}{\alpha} + \mathcal{O}(\varepsilon^2), \quad \underline{\alpha}(\varepsilon) = \varepsilon \underline{\overset{(1)}{\alpha}} + \mathcal{O}(\varepsilon^2), \quad \beta(\varepsilon) = \varepsilon \overset{(1)}{\beta} + \mathcal{O}(\varepsilon^2), \quad \underline{\beta}(\varepsilon) = \varepsilon \underline{\overset{(1)}{\beta}} + \mathcal{O}(\varepsilon^2), \quad \sigma(\varepsilon) = \varepsilon \overset{(1)}{\sigma} + \mathcal{O}(\varepsilon^2).$$

Here $\overset{(1)}{\Omega}$, $(\Omega \text{tr} \chi)$, $(\Omega \text{tr} \underline{\chi})$, $\overset{(1)}{\omega}$, $\underline{\overset{(1)}{\omega}}$, $\overset{(1)}{\rho}$, $\overset{(1)}{\sigma}$, $\overset{(1)}{K}$ are spacetime functions, $\overset{(1)}{\eta}$, $\underline{\overset{(1)}{\eta}}$, $\overset{(1)}{\beta}$, $\underline{\overset{(1)}{\beta}}$ are $S_{u,v}$ 1-forms, $\overset{(1)}{b}$ is an $S_{u,v}$ vector field, $\overset{(1)}{\not{g}}$ is an $S_{u,v}$ $(0,2)$ tensor, and $\overset{(1)}{\hat{\chi}}$, $\underline{\overset{(1)}{\hat{\chi}}}$, $\overset{(1)}{\hat{\alpha}}$, $\underline{\overset{(1)}{\hat{\alpha}}}$ are symmetric trace free $S_{u,v}$ $(0,2)$ tensor fields, of the fixed Schwarzschild background with respect to the Eddington–Finkelstein double null gauge of Example 3.1. The function r featuring in the Schwarzschild quantities is, as usual, the function $r(u,v)$ defined by (3.3).

The linearised induced metric $\overset{(1)}{\not{g}}$ is further decomposed into its trace and trace free parts, with respect to the round metric, as

$$\overset{(1)}{\not{g}}_{AB} = \overset{(1)}{\hat{g}}_{AB} + \frac{1}{2}(\overset{(1)}{\not{g}}_{\circ})_{AB} \cdot \text{tr}_{\overset{(1)}{\not{g}}_{\circ}} \overset{(1)}{\not{g}}, \quad \text{where } \text{tr}_{\overset{(1)}{\not{g}}_{\circ}} \overset{(1)}{\not{g}} = \overset{(1)}{\not{g}}_{\circ}^{CD} \overset{(1)}{\not{g}}_{CD}.$$

One then inserts these expansions into the null structure and Bianchi equations (3.25)–(3.51). The resulting system is satisfied to zeroth order in ε in view of the fact that Schwarzschild in Eddington–Finkelstein double null gauge is a solution. The linearised equations consist of the order ε part of the resulting system, and takes the following form. The linearised structure equations for the Ricci coefficients (3.25)–(3.38) take the form

$$\overset{(1)}{\nabla}_4(\Omega \text{tr} \chi) = \Omega_{\circ} \left(2d\overset{(1)}{v} \overset{(1)}{\eta} + 2\overset{(1)}{\rho} + 4\rho_{\circ} \Omega_{\circ}^{-1} \overset{(1)}{\Omega} \right) - \frac{1}{2} \text{tr} \chi_{\circ} \left((\Omega \text{tr} \underline{\chi}) - (\Omega \text{tr} \chi) \right), \quad (4.1)$$

$$\overset{(1)}{\nabla}_3(\Omega \text{tr} \chi) = \Omega_{\circ} \left(2d\overset{(1)}{v} \overset{(1)}{\eta} + 2\overset{(1)}{\rho} + 4\rho_{\circ} \Omega_{\circ}^{-1} \overset{(1)}{\Omega} \right) - \frac{1}{2} \text{tr} \chi_{\circ} \left((\Omega \text{tr} \underline{\chi}) - (\Omega \text{tr} \chi) \right), \quad (4.2)$$

$$\overset{(1)}{\nabla}_4(\Omega \text{tr} \underline{\chi}) = -\text{tr} \chi_{\circ} (\Omega \text{tr} \underline{\chi}) + 2\hat{\omega}(\Omega \text{tr} \underline{\chi}) + 2\text{tr} \chi_{\circ} \overset{(1)}{\hat{\omega}}, \quad \overset{(1)}{\nabla}_3(\Omega \text{tr} \underline{\chi}) = -\text{tr} \underline{\chi}_{\circ} (\Omega \text{tr} \underline{\chi}) + 2\underline{\hat{\omega}}(\Omega \text{tr} \underline{\chi}) + 2\text{tr} \underline{\chi}_{\circ} \overset{(1)}{\hat{\omega}}, \quad (4.3)$$

$$\overset{(1)}{\nabla}_3 \left(\Omega_{\circ}^{-1} \overset{(1)}{\hat{\chi}} \right) + \Omega_{\circ}^{-1} \text{tr} \underline{\chi}_{\circ} \overset{(1)}{\hat{\chi}} = -\Omega_{\circ}^{-1} \overset{(1)}{\hat{\alpha}}, \quad \overset{(1)}{\nabla}_4 \left(\Omega_{\circ}^{-1} \overset{(1)}{\hat{\chi}} \right) + \Omega_{\circ}^{-1} \text{tr} \chi_{\circ} \overset{(1)}{\hat{\chi}} = -\Omega_{\circ}^{-1} \overset{(1)}{\alpha}, \quad (4.4)$$

$$\overset{(1)}{\nabla}_3 \left(\Omega_{\circ} \overset{(1)}{\hat{\chi}} \right) + \frac{1}{2} (\Omega \text{tr} \underline{\chi})_{\circ} \overset{(1)}{\hat{\chi}} + \frac{1}{2} (\Omega \text{tr} \chi)_{\circ} \underline{\overset{(1)}{\hat{\chi}}} = -2\Omega_{\circ} \mathcal{P}_2^* \overset{(1)}{\eta}, \quad (4.5)$$

$$\overset{(1)}{\nabla}_4 \left(\Omega_{\circ} \overset{(1)}{\hat{\chi}} \right) + \frac{1}{2} (\Omega \text{tr} \chi)_{\circ} \overset{(1)}{\hat{\chi}} + \frac{1}{2} (\Omega \text{tr} \underline{\chi})_{\circ} \underline{\overset{(1)}{\hat{\chi}}} = -2\Omega_{\circ} \mathcal{P}_2^* \underline{\overset{(1)}{\eta}}. \quad (4.6)$$

$$\overset{(1)}{\nabla}_3 \overset{(1)}{\eta} = \frac{1}{2} \text{tr} \chi_{\circ} (\overset{(1)}{\eta} - \underline{\overset{(1)}{\eta}}) + \overset{(1)}{\beta}, \quad \overset{(1)}{\nabla}_4 \overset{(1)}{\eta} = -\frac{1}{2} \text{tr} \chi_{\circ} (\overset{(1)}{\eta} - \underline{\overset{(1)}{\eta}}) - \overset{(1)}{\beta}, \quad (4.7)$$

$$\overset{(1)}{\nabla}_4 \underline{\overset{(1)}{\eta}} = -\frac{1}{2} \text{tr} \chi_{\circ} \underline{\overset{(1)}{\eta}} + \overset{(1)}{\beta} + \frac{2}{\Omega_{\circ}} \overset{(1)}{\nabla} \overset{(1)}{\omega}, \quad \overset{(1)}{\nabla}_3 \underline{\overset{(1)}{\eta}} = -\frac{1}{2} \text{tr} \underline{\chi}_{\circ} \underline{\overset{(1)}{\eta}} - \overset{(1)}{\beta} + \frac{2}{\Omega_{\circ}} \overset{(1)}{\nabla} \underline{\overset{(1)}{\omega}}, \quad (4.8)$$

$$\overset{(1)}{\nabla}_4 \overset{(1)}{\omega} = -\overset{(1)}{\rho} - 2\rho_{\circ} \Omega_{\circ}^{-1} \overset{(1)}{\Omega}, \quad \overset{(1)}{\nabla}_3 \overset{(1)}{\omega} = -\overset{(1)}{\rho} - 2\rho_{\circ} \Omega_{\circ}^{-1} \overset{(1)}{\Omega}, \quad (4.9)$$

$$d\overset{(1)}{v} \overset{(1)}{\hat{\chi}} = -\frac{1}{2} \text{tr} \underline{\chi}_{\circ} \overset{(1)}{\eta} + \overset{(1)}{\beta} + \frac{1}{2\Omega_{\circ}} \overset{(1)}{\nabla} (\Omega \text{tr} \underline{\chi}), \quad d\overset{(1)}{v} \underline{\overset{(1)}{\hat{\chi}}} = -\frac{1}{2} \text{tr} \chi_{\circ} \underline{\overset{(1)}{\eta}} - \overset{(1)}{\beta} + \frac{1}{2\Omega_{\circ}} \overset{(1)}{\nabla} (\Omega \text{tr} \chi), \quad (4.10)$$

$$\text{curl}^{(i)}\eta = \overset{(i)}{\sigma}, \quad \text{curl}^{(i)}\underline{\eta} = -\overset{(i)}{\sigma}, \quad (4.11)$$

$$\overset{(i)}{K} = -\overset{(i)}{\rho} - \frac{1}{4} \frac{\text{tr}\chi_{\circ}}{\Omega_{\circ}} \left((\Omega \text{tr}\underline{\chi}) - (\Omega \text{tr}\chi) \right) + \frac{1}{2} \text{tr}\chi_{\circ} \text{tr}\underline{\chi}_{\circ} \Omega_{\circ}^{-1} \overset{(i)}{\Omega}, \quad (4.12)$$

the linearised Bianchi equations for the curvature components (3.39)–(3.48) take the form

$$\nabla_3 \overset{(i)}{\alpha} + \frac{1}{2} \text{tr}\underline{\chi}_{\circ} \overset{(i)}{\alpha} + 2\hat{\omega}_{\circ} \overset{(i)}{\alpha} = -2\mathcal{P}_2^* \overset{(i)}{\beta} - 3\rho_{\circ} \overset{(i)}{\chi}, \quad (4.13)$$

$$\nabla_4 \overset{(i)}{\beta} + 2\text{tr}\chi_{\circ} \overset{(i)}{\beta} - \hat{\omega}_{\circ} \overset{(i)}{\beta} = \text{div} \overset{(i)}{\alpha}, \quad (4.14)$$

$$\nabla_3 \overset{(i)}{\beta} + \text{tr}\underline{\chi}_{\circ} \overset{(i)}{\beta} + \hat{\omega}_{\circ} \overset{(i)}{\beta} = \nabla \overset{(i)}{\rho} + * \nabla \overset{(i)}{\sigma} + 3\rho_{\circ} \overset{(i)}{\eta}, \quad (4.15)$$

$$\nabla_4 \overset{(i)}{\rho} + \frac{3}{2} \text{tr}\chi_{\circ} \overset{(i)}{\rho} = \text{div} \overset{(i)}{\beta} - \frac{3}{2} \frac{\rho_{\circ}}{\Omega_{\circ}} (\Omega \text{tr}\chi), \quad (4.16)$$

$$\nabla_3 \overset{(i)}{\rho} + \frac{3}{2} \text{tr}\underline{\chi}_{\circ} \overset{(i)}{\rho} = -\text{div} \overset{(i)}{\underline{\beta}} - \frac{3}{2} \frac{\rho_{\circ}}{\Omega_{\circ}} (\Omega \text{tr}\underline{\chi}), \quad (4.17)$$

$$\nabla_4 \overset{(i)}{\sigma} + \frac{3}{2} \text{tr}\chi_{\circ} \overset{(i)}{\sigma} = -\text{curl} \overset{(i)}{\beta}, \quad (4.18)$$

$$\nabla_3 \overset{(i)}{\sigma} + \frac{3}{2} \text{tr}\underline{\chi}_{\circ} \overset{(i)}{\sigma} = -\text{curl} \overset{(i)}{\underline{\beta}}, \quad (4.19)$$

$$\nabla_4 \overset{(i)}{\underline{\beta}} + \text{tr}\chi_{\circ} \overset{(i)}{\underline{\beta}} + \hat{\omega}_{\circ} \overset{(i)}{\underline{\beta}} = -\nabla \overset{(i)}{\rho} + * \nabla \overset{(i)}{\sigma} - 3\rho_{\circ} \overset{(i)}{\underline{\eta}}, \quad (4.20)$$

$$\nabla_3 \overset{(i)}{\underline{\beta}} + 2\text{tr}\underline{\chi}_{\circ} \overset{(i)}{\underline{\beta}} - \hat{\omega}_{\circ} \overset{(i)}{\underline{\beta}} = -\text{div} \overset{(i)}{\underline{\alpha}}, \quad (4.21)$$

$$\nabla_4 \overset{(i)}{\underline{\alpha}} + \frac{1}{2} \text{tr}\chi_{\circ} \overset{(i)}{\underline{\alpha}} + 2\hat{\omega}_{\circ} \overset{(i)}{\underline{\alpha}} = 2\mathcal{P}_2^* \overset{(i)}{\underline{\beta}} - 3\rho_{\circ} \overset{(i)}{\underline{\chi}}, \quad (4.22)$$

and the linearised equations for the metric components (3.49)–(3.51) take the form

$$e_3 \left(\text{tr}_{\hat{\mathcal{G}}_{\circ}} \overset{(i)}{\hat{\mathcal{G}}} \right) = 2(\Omega \text{tr}\underline{\chi}), \quad e_4 \left(\text{tr}_{\hat{\mathcal{G}}_{\circ}} \overset{(i)}{\hat{\mathcal{G}}} \right) = 2(\Omega \text{tr}\chi) - 2\text{div} \overset{(i)}{b}, \quad (4.23)$$

$$\sqrt{\hat{\mathcal{G}}_{\circ}} \Omega_{\circ} e_3 \left(\frac{\overset{(i)}{\hat{\mathcal{G}}_{AB}}}{\sqrt{\hat{\mathcal{G}}_{\circ}}} \right) = 2\Omega_{\circ} \overset{(i)}{\hat{\chi}}_{AB}, \quad \sqrt{\hat{\mathcal{G}}_{\circ}} \Omega_{\circ} e_4 \left(\frac{\overset{(i)}{\hat{\mathcal{G}}_{AB}}}{\sqrt{\hat{\mathcal{G}}_{\circ}}} \right) = 2\Omega_{\circ} \overset{(i)}{\hat{\chi}}_{AB} + 2 \left(\mathcal{P}_2^* \overset{(i)}{b} \right)_{AB}, \quad (4.24)$$

$$\partial_u \overset{(i)}{b}^A = 2\Omega_{\circ}^2 \left(\overset{(i)}{\eta}^A - \overset{(i)}{\underline{\eta}}^A \right), \quad (4.25)$$

$$\overset{(i)}{\omega} = e_4 \left(\Omega_{\circ}^{-1} \overset{(i)}{\Omega} \right), \quad \overset{(i)}{\underline{\omega}} = e_3 \left(\Omega_{\circ}^{-1} \overset{(i)}{\Omega} \right), \quad \overset{(i)}{\eta} + \overset{(i)}{\underline{\eta}} = 2\nabla \left(\Omega_{\circ}^{-1} \overset{(i)}{\Omega} \right). \quad (4.26)$$

See Section 5 of [19] for more details of the formal linearisation procedure. Finally, it is noted that the linearised system (4.1)–(4.26) admits a well posed Cauchy and characteristic initial value problem. See Theorem 8.1 of [19].

4.2 Residual pure gauge and linearised Kerr families of solutions

The problem of linear stability of Schwarzschild involves showing that solutions of the linearised system (4.1)–(4.26) remain uniformly bounded and decay in time. The problem is complicated by the existence of two special *non-decaying* families of solutions.

The first non-decaying family is infinite dimensional, and arises from the infinite dimensional family of residual freedom in double null gauge (see Remark 3.2). This family is thus called the family of *pure gauge solutions*.

Proposition 4.2 (A family of pure gauge solutions). *For any functions $f^3(u, \theta^1, \theta^2)$, $f^4(v, \theta^1, \theta^2)$, the linearised metric quantities*

$$2\Omega_{\circ}^{-1}{}^{(v)}\Omega = \partial_u f^3 + \partial_v f^4 - \frac{2M}{r^2}(f^3 - f^4), \quad \hat{g}^{(v)} = -\frac{4}{r}r^2\mathcal{P}_2^*\nabla f^4, \quad \text{tr}_{\hat{g}_{\circ}}{}^{(v)}\hat{g} = \frac{4\Omega_{\circ}^2}{r}(f^4 - f^3) + \frac{4}{r}r^2\Delta f^4, \\ \hat{b} = (2\Omega_{\circ}^2\nabla(f^3 + f^4) + 2r\nabla\partial_v f^4)^{\sharp},$$

the linearised Ricci coefficients

$$\hat{\chi}^{(v)} = -2\Omega_{\circ}\mathcal{P}_2^*\nabla f^3, \quad \hat{\underline{\chi}}^{(v)} = -2\Omega_{\circ}\mathcal{P}_2^*\nabla f^4, \\ (\Omega\text{tr}\chi)^{(v)} = \frac{2\Omega_{\circ}^2}{r}\partial_v f^4 + 2\Omega_{\circ}^2\Delta f^3 + \frac{2\Omega_{\circ}^2}{r^2}\left(1 - \frac{4M}{r}\right)(f^3 - f^4), \\ (\Omega\text{tr}\underline{\chi})^{(v)} = -\frac{2\Omega_{\circ}^2}{r}\partial_u f^3 + 2\Omega_{\circ}^2\Delta f^4 - \frac{2\Omega_{\circ}^2}{r^2}\left(1 - \frac{4M}{r}\right)(f^3 - f^4), \\ \hat{\eta}^{(v)} = \nabla\partial_u f^3 + (2\Omega\hat{\omega}_{\circ} - \frac{1}{2}\Omega\text{tr}\chi_{\circ})\nabla f^3 + \frac{1}{2}\Omega\text{tr}\chi_{\circ}\nabla f^4, \\ \hat{\underline{\eta}}^{(v)} = \nabla\partial_v f^4 + (2\Omega\hat{\omega}_{\circ} - \frac{1}{2}\Omega\text{tr}\chi_{\circ})\nabla f^4 + \frac{1}{2}\Omega\text{tr}\chi_{\circ}\nabla f^3, \\ \hat{\omega}^{(v)} = \frac{1}{2}\partial_v^2 f^4 + \frac{M}{r^2}\partial_v f^4 + \frac{2M}{r^3}\Omega_{\circ}^2(f^3 - f^4), \quad \hat{\underline{\omega}}^{(v)} = \frac{1}{2}\partial_u^2 f^3 - \frac{M}{r^2}\partial_u f^3 - \frac{2M}{r^3}\Omega_{\circ}^2(f^3 - f^4),$$

and the linearised curvature components

$$\hat{\alpha}^{(v)} = 0, \quad \hat{\underline{\alpha}}^{(v)} = 0, \quad \hat{\beta}^{(v)} = -\frac{6M\Omega_{\circ}}{r^3}\nabla f^3, \quad \hat{\underline{\beta}}^{(v)} = \frac{6M\Omega_{\circ}}{r^3}\nabla f^4, \quad \hat{\rho}^{(v)} = \frac{6M\Omega_{\circ}^2}{r^4}(f^4 - f^3), \quad \hat{\sigma}^{(v)} = 0,$$

define a solution of the linearised system (4.1)–(4.26), called a pure gauge solution.

See Section 6 of [19] for the most general family of pure gauge solutions (the pure gauge solutions of Proposition 4.2 correspond to those of Lemma 6.1.1 and Lemma 6.1.2 of [19]). One arrives at the expressions of Proposition 4.2 by noting that transformations of the form

$$\mathbf{u}_{\varepsilon} = u + \varepsilon f^3(u, \theta^1, \theta^2), \quad \mathbf{v}_{\varepsilon} = v + \varepsilon f^4(v, \theta^1, \theta^2), \quad \boldsymbol{\theta}_{\varepsilon}^A = \theta^A + \varepsilon 2r\mathcal{g}^{AB}\partial_B f^4(v, \theta^1, \theta^2),$$

preserve the double null form of the metric to linear order, and computing the change in linearised metric components, Ricci coefficients, and curvature components with respect to such a change.

The second non-decaying family is finite dimensional, and arises from the presence of members of the Kerr family (1.3). This non-decaying family of solutions of the linearised equations can be divided into a one dimension family of *linearised Schwarzschild solutions*, and a three dimensional family of *fixed mass linearised Kerr solutions*.⁴

⁴Given that Kerr is a two parameter family of solutions of (1.2), one might expect the linearised Kerr family to be two dimensional. The high degrees of symmetry possessed by Schwarzschild, however, mean that, in order to parameterise smoothly, it is convenient to over count. One can view the numerology as arising from the fact that, given a member of Schwarzschild, to describe a nearby member of the Kerr family one not only needs to choose a mass and angular momentum parameter, but also an axis around which the Kerr member is rotating. The mass and angular momentum parameters, together with the axis of rotation, constitute four parameters in total.

Proposition 4.3 (The family of linearised Kerr solutions). *For any parameter \mathbf{m} , the quantities*

$$2\Omega_{\circ}^{-1} \overset{(\circ)}{\Omega} = -\mathbf{m}, \quad \overset{(\circ)}{\not{g}} = -2\mathbf{m}\not{g}_{\circ}, \quad \overset{(\circ)}{\rho} = -\frac{2M}{r^3}\mathbf{m}, \quad \overset{(\circ)}{K} = \frac{\mathbf{m}}{r^2}, \quad (4.27)$$

$$\overset{(\circ)}{\beta} = (\Omega \text{tr} \chi) = (\Omega \text{tr} \underline{\chi}) = \overset{(\circ)}{\omega} = \overset{(\circ)}{\underline{\omega}} = \overset{(\circ)}{\sigma} = \overset{(\circ)}{\eta} = \overset{(\circ)}{\underline{\eta}} = \overset{(\circ)}{\beta} = \overset{(\circ)}{\underline{\beta}} = \overset{(\circ)}{\hat{\chi}} = \overset{(\circ)}{\underline{\hat{\chi}}} = \overset{(\circ)}{\alpha} = \overset{(\circ)}{\underline{\alpha}} = 0, \quad (4.28)$$

define a spherically symmetric solution of the linearised system (4.1)–(4.26), called a linearised Schwarzschild solution. For any parameters \mathbf{a}^{-1} , \mathbf{a}^0 , \mathbf{a}^1 , the quantities

$$\overset{(\circ)}{\sigma} = \sum_{m=-1}^1 \mathbf{a}^m \frac{6}{r^4} Y_m^{\ell=1}, \quad \overset{(\circ)}{\eta} = -\overset{(\circ)}{\underline{\eta}} = \sum_{m=-1}^1 \mathbf{a}^m \frac{3}{r^2} * \not{\nabla} Y_m^{\ell=1}, \quad \overset{(\circ)}{b} = \sum_{m=-1}^1 \mathbf{a}^m \frac{4}{r} * \not{\nabla} Y_m^{\ell=1}, \quad (4.29)$$

$$\overset{(\circ)}{\underline{\beta}} = -\Omega_{\circ} \sum_{m=-1}^1 \mathbf{a}^m \frac{3}{r^3} * \not{\nabla} Y_m^{\ell=1}, \quad \overset{(\circ)}{\beta} = \Omega_{\circ} \sum_{m=-1}^1 \mathbf{a}^m \frac{3}{r^3} * \not{\nabla} Y_m^{\ell=1}, \quad (4.30)$$

$$\overset{(\circ)}{\Omega} = \overset{(\circ)}{\not{g}} = \overset{(\circ)}{\rho} = \overset{(\circ)}{K} = (\Omega \text{tr} \chi) = (\Omega \text{tr} \underline{\chi}) = \overset{(\circ)}{\omega} = \overset{(\circ)}{\underline{\omega}} = \overset{(\circ)}{\hat{\chi}} = \overset{(\circ)}{\underline{\hat{\chi}}} = \overset{(\circ)}{\alpha} = \overset{(\circ)}{\underline{\alpha}} = 0, \quad (4.31)$$

define a solution of the linearised system (4.1)–(4.26), called a fixed mass linearised Kerr solution. Here $Y_{-1}^{\ell=1}$, $Y_0^{\ell=1}$, $Y_1^{\ell=1}$ denote the $\ell = 1$ spherical harmonics. In (θ, ϕ) coordinates,

$$Y_{-1}^{\ell=1}(\theta, \phi) = \sqrt{\frac{3}{4\pi}} \sin \theta \sin \phi, \quad Y_0^{\ell=1}(\theta, \phi) = \sqrt{\frac{3}{4\pi}} \cos \theta, \quad Y_1^{\ell=1}(\theta, \phi) = \sqrt{\frac{3}{4\pi}} \sin \theta \cos \phi.$$

Note that the linearised Schwarzschild family (4.27)–(4.28) is supported on the $\ell = 0$ spherical harmonic, and the fixed mass linearised Kerr family (4.29)–(4.31) is supported on the $\ell = 1$ spherical harmonics. (See Section 4.4.2 of [19] for a discussion of what it means for $S_{u,v}$ -1 forms and symmetric trace free $(0, 2)$ $S_{u,v}$ -tensors to be supported on $\ell = 0$ and $\ell = 1$.)

Linear stability of Schwarzschild then involves showing that solutions of the linearised system (4.1)–(4.26) remain uniformly bounded, and moreover decay in time to a member of the family of pure gauge solutions, plus a member of the family of linearised Kerr solutions.

4.3 The linear stability theorem

Theorem 4.1 can now be more precisely stated as follows. Consider the initial hypersurfaces $C_0 = \{u = 0\}$ and $\underline{C}_0 = \{v = 0\}$ in Schwarzschild, defined with respect to the Eddington–Finkelstein double null gauge.

Theorem 4.4 (Linear stability of Schwarzschild in double null gauge [19]). *For any initial data for the linearised Einstein equations (4.1)–(4.26) on $C_0 \cup \underline{C}_0$, which satisfies appropriate initial gauge conditions on $C_0 \cup \underline{C}_0$ (see Definition 9.1 of [19]), the resulting solution*

1. *Remains uniformly bounded in the exterior by initial data;*
2. *Decays, at an inverse polynomial rate, to a member of the linearised Kerr family, after adding a residual pure gauge solution.*

Moreover, the residual pure gauge solution which is added is uniformly controlled by initial data.

The boundedness and decay of Theorem 4.4 hold up to and including the event horizon \mathcal{H}^+ , and the decay to the linearised Kerr solution in particular holds along \mathcal{I}^+ and \mathcal{H}^+ .

Recall (see the brief discussion in Section 1) that the notion of a black hole is *teleological*. The black hole exterior of a spacetime is characterised as the causal past of an appropriate complete future null infinity \mathcal{I}^+ . In the context of Theorem 1.1, this means that, at the level of initial data, it is impossible in general to a priori characterise the black hole exterior exactly (assuming that the resulting solution indeed contains a black hole) as it in general depends on how the solution behaves in evolution. By a miracle of linear

theory, however, the linearised analogue of the black hole exterior of the linear perturbations of Theorem 4.4 *can* be characterised explicitly in terms of initial data (see Section 4.5 below for a further discussion). Moreover, the member of the linearised Kerr family to which the solution in Theorem 4.4 decays is also explicitly characterised. Contrast with Theorem 1.1, in which the black hole exterior and the codimension 3 submanifold are characterised teleologically as part of the proof. See the discussion in Section 5 below for the resulting additional complications in the proof of Theorem 1.1.

In contrast, the characterisation of the normalisation of the residual pure gauge freedom required to decay to Schwarzschild in the Eddington–Finkelstein double null gauge of Example 3.1 is *already teleological in the linearised setting of Theorem 4.4*. See Section 4.5 below for a discussion of the dependence of the pure gauge solution of Theorem 4.4 on the behaviour of the solution in evolution.

In view of the fact that every solution of Theorem 4.4 decays to a member of the linearised Kerr family, it is perhaps more appropriate to call Theorem 4.4 the *linear stability of the Kerr family around Schwarzschild*. Since the member of the linearised Kerr family to which the solution decays is determined explicitly in terms of initial data, one can immediately infer the following Corollary of Theorem 4.4, which should be viewed as the linearised analogue of Theorem 1.1.

Corollary 4.5 (Full finite codimension stability of linearised Schwarzschild family around Schwarzschild). *There exists a codimension-3 subspace of initial data for the linearised Einstein equations (4.1)–(4.26) for which the resulting solution decays to a member of the linearised Schwarzschild family.*

In the remainder of this section the proof of Theorem 4.4 is outlined.

4.4 Boundedness and decay for solutions of the Teukolsky equation

The first advantage of double null gauge at the linear level is that it allows one to apply insights from the Newman–Penrose formalism [57]. Indeed, a natural starting point in the analysis of the linearised system (4.1)–(4.26) is the curvature components $\overset{\circ}{\alpha}$ and $\overset{\circ}{\underline{\alpha}}$. As was first observed by Bardeen–Press [5], these curvature components satisfy decoupled wave equations.

Proposition 4.6 (Teukolsky equations). *Consider a solution of the linearised system (4.1)–(4.26). The linearised curvature component $\overset{\circ}{\alpha}$ satisfies the decoupled equation*

$$-\Omega_{\circ}\nabla_4\Omega_{\circ}\nabla_3(r\Omega_{\circ}^2\overset{\circ}{\alpha}) + \Omega_{\circ}^2\Delta(r\Omega_{\circ}^2\overset{\circ}{\alpha}) - \frac{4}{r}\left(1 - \frac{3M}{r}\right)\Omega_{\circ}\nabla_3(r\Omega_{\circ}^2\overset{\circ}{\alpha}) - \frac{2\Omega_{\circ}^2}{r^2}\left(1 + \frac{3M}{r}\right)r\Omega_{\circ}^2\overset{\circ}{\alpha} = 0, \quad (4.32)$$

and the curvature component $\overset{\circ}{\underline{\alpha}}$ satisfies

$$-\Omega_{\circ}\nabla_3\Omega_{\circ}\nabla_4(r\Omega_{\circ}^2\overset{\circ}{\underline{\alpha}}) + \Omega_{\circ}^2\Delta(r\Omega_{\circ}^2\overset{\circ}{\underline{\alpha}}) + \frac{4}{r}\left(1 - \frac{3M}{r}\right)\Omega_{\circ}\nabla_4(r\Omega_{\circ}^2\overset{\circ}{\underline{\alpha}}) - \frac{2\Omega_{\circ}^2}{r^2}\left(1 + \frac{3M}{r}\right)r\Omega_{\circ}^2\overset{\circ}{\underline{\alpha}} = 0. \quad (4.33)$$

Proof. Consider first equation (4.32). Note the commutation relations

$$[\Omega_{\circ}\nabla_3, \Omega_{\circ}\nabla_4] = [\Omega_{\circ}\nabla_3, r\mathcal{D}_2^*] = [\Omega_{\circ}\nabla_4, r\mathcal{D}_2^*] = 0, \quad (4.34)$$

and the fact that

$$\partial_u r = -\left(1 - \frac{2M}{r}\right), \quad \partial_v r = \left(1 - \frac{2M}{r}\right). \quad (4.35)$$

Equations (4.13), (4.14) and the latter of (4.4) can be rewritten

$$\frac{r^4}{\Omega_{\circ}^4}\Omega_{\circ}\nabla_3(r\Omega_{\circ}^2\overset{\circ}{\alpha}) = -2r\mathcal{D}_2^*(r^4\Omega_{\circ}^{-1}\overset{\circ}{\beta}) + 6Mr^2\Omega_{\circ}^{-1}\overset{\circ}{\chi}, \quad (4.36)$$

$$\Omega_{\circ}\nabla_4(r^4\Omega_{\circ}^{-1}\overset{\circ}{\beta}) = r^4\mathcal{D}_4\overset{\circ}{\alpha}, \quad (4.37)$$

$$\Omega_{\circ}\nabla_4\left(r^2\Omega_{\circ}^{-1}\overset{\circ}{\chi}\right) = -r^2\overset{\circ}{\alpha}, \quad (4.38)$$

respectively. Applying $\Omega_{\circ}\nabla_4$ to (4.36), it follows that

$$\Omega_{\circ}\nabla_4(\Omega_{\circ}^{-4}r^4\Omega_{\circ}\nabla_3(r\Omega_{\circ}^2\overset{\circ}{\alpha})) = -2r^5\mathcal{D}_2^*\mathfrak{d}\overset{\circ}{\nu}\alpha - 6Mr^2\alpha.$$

Equation (4.32) follows from noting that

$$\partial_v(\Omega_{\circ}^{-4}r^4) = \frac{r^4}{\Omega^4} \frac{4}{r} \left(1 - \frac{3M}{r}\right),$$

and

$$\mathcal{D}_2^*\mathfrak{d}\overset{\circ}{\nu}\alpha = -\frac{1}{2}\mathfrak{A}\overset{\circ}{\alpha} + \frac{1}{r^2}\overset{\circ}{\alpha}.$$

Equation (4.33) follows similarly, using now equations (4.21), (4.22), and the former of (4.4). \square

Analogous decoupled wave equations to (4.32) and (4.33) can be derived for the linearised Einstein equations around Kerr (provided $\overset{\circ}{\alpha}$ and $\overset{\circ}{\underline{\alpha}}$ are defined with respect to an appropriate *algebraically special frame*), as was shown by Teukolsky [65]. Equations (4.32) and (4.33) are thus referred to as the *Teukolsky equations*.

Moreover, $\overset{\circ}{\alpha}$ and $\overset{\circ}{\underline{\alpha}}$ are *gauge invariant*, meaning that they remain unchanged under the addition of a residual pure gauge solution of Proposition 4.2 or linearised Kerr solution of Proposition 4.3 (and, conversely, any admissible solution with $\overset{\circ}{\alpha} = \overset{\circ}{\underline{\alpha}} = 0$ is necessarily the sum of a pure gauge and linearised Kerr solution), and thus they can be studied independently of how the residual double null freedom is normalised.

It is difficult to analyse solutions of the Teukolsky equations (4.32) and (4.33) directly, in view of their first order terms. It was not known how to show boundedness and decay properties of solutions, beyond statements about fixed frequency solutions, until the work [19].

Theorem 4.7 (Boundedness and decay for solutions of the Teukolsky equation [19]). *Solutions of the Teukolsky equations (4.32) and (4.33) on the Schwarzschild exterior, arising from regular localised initial data, remain uniformly bounded, and decay in time at an inverse polynomial rate.*

The reader is referred to Theorem 2 of [19] for a more precise statement (which in particular includes top order boundedness without loss of derivatives). Theorem 4.7 has moreover been generalised to Kerr in the very slowly rotating $|a| \ll M$ case [17], [54], and to the full subextremal range $|a| < M$ [62].

The proof of Theorem 4.7 proceeds by considering the following transformed quantities

$$\overset{\circ}{P} = -\frac{1}{2}r^{-3}\Omega_{\circ}^{-1}\nabla_3(r^2\Omega_{\circ}^{-1}\nabla_3(r\Omega_{\circ}^2\overset{\circ}{\alpha})), \quad \overset{\circ}{\underline{P}} = -\frac{1}{2}r^{-3}\Omega_{\circ}^{-1}\nabla_4(r^2\Omega_{\circ}^{-1}\nabla_4(r\Omega_{\circ}^2\overset{\circ}{\underline{\alpha}})). \quad (4.39)$$

These quantities satisfy the *Regge–Wheeler equation*.

Proposition 4.8 (Regge–Wheeler equation). *For any solutions $\overset{\circ}{\alpha}$ and $\overset{\circ}{\underline{\alpha}}$ of the Teukolsky equations (4.32), (4.33), the quantities $\overset{\circ}{P}$ and $\overset{\circ}{\underline{P}}$ defined by (4.39) satisfy the Regge–Wheeler equation*

$$-\Omega_{\circ}\nabla_4\Omega_{\circ}\nabla_3(r^5\overset{\circ}{P}) + \left(1 - \frac{2M}{r}\right)\mathfrak{A}(r^5\overset{\circ}{P}) - \left(\frac{4}{r^2} - \frac{6M}{r^3}\right)\left(1 - \frac{2M}{r}\right)r^5\overset{\circ}{P} = 0. \quad (4.40)$$

Proof. The proof uses the commutation relations (4.34) and the fact (4.35), and is left as an exercise to the reader. See also Section 3.4 of [20] for the analogous derivation in a nonlinear setting. \square

Equation (4.40) first arose in the work of Regge–Wheeler [60] in the context of the so-called metric perturbations approach, where it governed, however, only “half” of the gauge invariant part of the perturbations. It is remarkable that the very same equation is satisfied by the higher order quantities (4.39). The relations (4.39) are physical space reformulations of fixed frequency transformations originally discovered by Chandrasekhar [9].

In contrast to the Teukolsky equations (4.32) and (4.33), the Regge–Wheeler equation can be analysed in much the same way as the standard linear wave equation (2.1) (note in particular the absence of terms involving first order derivatives of $\overset{\circ}{P}$ in (4.40)). In particular, the methods described in Section 2 yield appropriate boundedness and decay statements for solutions of (4.40). The proof of Theorem 4.7 concludes by inverting the transformations (4.39) to obtain boundedness and decay properties of $\overset{\circ}{\alpha}$ and $\overset{\circ}{\underline{\alpha}}$.

4.5 Boundedness and decay for the remainder of the linearised system

The remainder of the proof of Theorem 4.4 concerns the remaining, gauge dependent, part of the linearised system (4.1)–(4.26).

4.5.1 The initial gauge normalisation and fixed Kerr modes

In the study of this gauge dependent part of the system, the first task is to normalise the residual double null freedom to initial data. In linear theory this normalisation corresponds to adding a pure gauge solution, so that certain quantities are fixed initially. For example, one can arrange to fix the quantity

$$(\Omega \text{tr} \chi)|_{S_{\infty,0}} = 0, \quad (4.41)$$

at the initial sphere $(u, v) = (\infty, 0)$ of the event horizon \mathcal{H}^+ . It turns out that this condition is then preserved along \mathcal{H}^+ under evolution by the linearised system (4.1)–(4.26). The condition (4.41) can thus be thought of as ensuring that the “location of the event horizon” of the linear perturbation coincides with the location of the event horizon of the background Schwarzschild spacetime. Since the vanishing of $(\Omega \text{tr} \chi)$ along all of \mathcal{H}^+ can be achieved with an *initial normalisation*, in contrast to the nonlinear problem of Theorem 1.1, the characterisation of the black hole exterior is not teleological in linear theory.

The $\ell = 0$ and $\ell = 1$ spherical harmonic modes of the linearised solution play an anomalous role in Theorem 4.4, and in particular in the initial gauge normalisation. It turns out that solutions supported only on $\ell = 0$ and $\ell = 1$ can be written as the sum of a pure gauge solution (see Proposition 4.2) and a linearised Kerr solution (see Proposition 4.3).⁵ Thus, by adding a pure gauge solution so as to fix certain quantities at the initial sphere $(u, v) = (\infty, 0)$ of \mathcal{H}^+ , for example

$$\Omega_o^{-2} (\Omega \text{tr} \underline{\chi})_{\ell=0,1}|_{S_{\infty,0}} = 0, \quad (\dot{\rho} + \text{div} \dot{\eta})_{\ell=1}|_{S_{\infty,0}} = 0, \quad (4.42)$$

the $\ell = 0$ and $\ell = 1$ part of the linearised solution will consist only of a linearised Kerr solution. This is precisely the linearised Kerr solution of Theorem 4.4, which can thus be explicitly determined by initial data. Thus, in contrast to the nonlinear problem of Theorem 1.1, the linearised Kerr solution of Theorem 4.4, or the codimension-3 subspace of Corollary 4.5, are not teleological.

See Definition 9.1 of [19] for a complete list of *initial gauge conditions*, which include the conditions (4.41) and (4.42).

4.5.2 Boundedness of the remaining quantities in the initial normalised gauge

If one considers the linearised curvature components $\overset{(i)}{\underline{\alpha}}$ and $\overset{(i)}{\underline{\beta}}$ as given inhomogeneous terms in the linearised system (4.1)–(4.26), then (4.1)–(4.26) can be viewed as a coupled system of transport and elliptic equations for the remaining part of the linearised solution. Moreover, there is a hierarchical structure present, which means that the system effectively decouples. For example, if $\overset{(i)}{\underline{\alpha}}$ is considered as a given inhomogeneous term then the former of equation (4.4) can be viewed as a transport equation for the quantity $\overset{(i)}{\underline{\chi}}$. If one then additionally considers $\overset{(i)}{\underline{\chi}}$ as an inhomogeneous term, then equation (4.22) can be viewed as an elliptic equation for the curvature component $\overset{(i)}{\underline{\beta}}$, and so on.

The boundedness part of Theorem 4.4 involves integrating these transport equations, in this hierarchical manner, forwards from the initial hypersurfaces $C_0 \cup \underline{C}_0$, where the initial normalisation, discussed in Section 4.5.1, provides appropriate initial conditions. In general, without teleologically renormalising the residual pure gauge freedom, this bounded statement is sharp, i.e. the solution does not decay. This fact can be illustrated already in the first step of the hierarchy when $\overset{(i)}{\underline{\chi}}$ is controlled.

⁵Note that the quantities $\overset{(i)}{\underline{\alpha}}$ and $\overset{(i)}{\underline{\beta}}$, which parameterise the gauge invariant part of the linearised solution, are symmetric trace free $(0, 2)$ $S_{u,v}$ -tensors, and can thus appropriately be viewed as having vanishing $\ell = 0$ and $\ell = 1$ spherical harmonics. See Proposition 4.4.1 of [19].

Recall equation (4.4) satisfied by $\underline{\hat{\chi}}^{(i)}$. There is already an issue in obtaining boundedness of $\underline{\hat{\chi}}^{(i)}$ in view of the fact that the appropriate integrating factor for equation (4.4), yielding

$$\nabla_3(r^2\Omega_o^{-1}\underline{\hat{\chi}}^{(i)}) = -r^2\Omega_o^{-1}\underline{\hat{\alpha}},$$

would require one to estimate $r^2\underline{\hat{\chi}}^{(i)}$ initially, which is however in general unbounded along the initial cone C_0 . One resolves this issue by introducing an auxiliary renormalised quantity

$$\underline{Y}^{(i)} = r^2\mathcal{D}_2^*\nabla(r^{-1}\Omega_o\underline{\hat{\chi}}^{(i)}) - \frac{1}{2}r^3\Omega_o^{-3}\nabla_4(r\Omega_o^2\underline{\hat{\alpha}}),$$

which can be shown to be bounded initially, and satisfies a transport equation without integrating factor and with integrable right hand side

$$\nabla_3\underline{Y}^{(i)} = -\frac{1}{2}r^2\Omega_o^{-2}\nabla_4(r\Omega_o^2\underline{\hat{\alpha}}) + 3M\Omega_o^{-1}r\underline{\hat{\alpha}}. \quad (4.43)$$

Integration of (4.43) from C_0 now indeed gives rise to a finite bound for $\underline{Y}^{(i)}$, and thus for $\underline{\hat{\chi}}^{(i)}$, but this bound is dominated at large v values by a flux associated to $\underline{\hat{\alpha}}$ which in general will be non-zero. Thus $\underline{Y}^{(i)}$, and consequently $\underline{\hat{\chi}}^{(i)}$, does not, in general, decay in this initial normalised gauge.

See [19] for a discussion of further difficulties which arise in establishing the boundedness part of Theorem 4.4, including the fact that the outgoing shear $\hat{\chi}$ is subject to a *blueshift*, and thus further properties of the redshift effect discussed in Section 2.1 have to be exploited.

4.5.3 Decay of the remaining quantities in the teleological gauge

In order for $\underline{Y}^{(i)}$, and hence $\underline{\hat{\chi}}^{(i)}$, to decay, one must renormalise the residual double null freedom in way dependent on how the solution has behaved in evolution. In the context of the linear theory, such a teleological normalisation amounts to adding a pure gauge solution related to the original solution (i.e. in the ‘‘initial data normalised gauge’’) by its value *somewhere to the future*, so as to normalise certain quantities to vanish there.

It turns out to be sufficient for our purposes here to require that the linearised metric quantity $\Omega_o^{-1}\underline{\hat{\Omega}}^{(i)}$ vanish identically *along the entire event horizon \mathcal{H}^+* :

$$\Omega_o^{-1}\underline{\hat{\Omega}}^{(i)} = 0, \quad \text{on } \mathcal{H}^+. \quad (4.44)$$

Relation (4.44) can indeed be arranged by adding a pure gauge solution (at the expense of relaxing a previous similar normalisation along the initial cone C_{out}). Moreover, in view of the boundedness statement just obtained, the pure gauge solution that must be added *is itself quantitatively bounded from initial data*.

One can now revisit the integration of the transport equation (4.43) for $\underline{Y}^{(i)}$ and integrate *backwards*, with the condition (4.44) along \mathcal{H}^+ ensuring that the *future* boundary terms are controlled. This allows one to indeed inherit decay properties from those already obtained for the gauge invariant quantities.

Combining the process again with the r^p -weighted energy hierarchy of [25], this allows one to obtain inverse polynomial decay for all quantities, completing the proof of Theorem 4.4.

Finally, it should be emphasised that the fact that the added pure gauge solution which assured (4.44) can itself be quantitatively bounded is fundamental for the nonlinear stability proof to be discussed in Section 5.

5 The nonlinear stability of the Schwarzschild family

The strategy of the proof of Theorem 1.1 is, in its broad outline, an adaptation of the linear stability analysis of [19] described in Section 4. Insights developed in the previous study of nonlinear problems, most notably the stability of Minkowski space [15], are adapted to control nonlinear terms. In addition, there are a number of nonlinear difficulties specific to Theorem 1.1. Examples of such difficulties are:

- Identification of the codimension 3 submanifold: The perturbations of Theorem 1.1 are confined to live on a codimension 3 “submanifold” of the moduli space of initial data. This codimension 3 “submanifold” consists of initial data which contain exactly the amount of angular momentum that the corresponding solutions radiate in evolution. In general there is no a priori way to determine how much angular momentum a solution will radiate in evolution (contrast with the linear theory of Section 4) and thus the “submanifold” is only characterised teleologically. See Section 5.3 below.
- Further normalisation of the residual gauge freedom: As in the linear theory of Section 4, in order for the solution to converge to Schwarzschild *in the Eddington–Finkelstein gauge of Example 3.1*, the residual double null freedom must be normalised teleologically. The proof of Theorem 5.2 in fact employs two distinct double null gauges, corresponding to a “near” region, where the redshift effect is relevant, and a “far” region, where the *null condition* is paramount. The null condition is a special structure in the nonlinearity of the Einstein equations (1.2), which one crucially has to exploit in nonlinear stability problems. See the discussion of the stability of Minkowski space in Section 5.1.
- Estimating nonlinear terms: In view of the degeneration of the top order integrated local energy decay estimates around the $r = 3M$ (see Proposition 2.9) and the discussion of the null condition in Section 5.1 below, estimating nonlinear terms is particularly nontrivial around the photon sphere and towards future null infinity. See Section 5.6 below.

5.1 The null condition and the nonlinear stability of Minkowski space

Before proceeding to describe the proof of Theorem 1.1, the relevant aspects of the stability of Minkowski space are briefly reviewed. In short, the proof of the stability of Minkowski space in $3 + 1$ dimensions relies crucially on exploiting the very special *null condition* present in the nonlinearity of the vacuum Einstein equations (1.2). Exploiting the null condition is also a fundamental aspect of Theorem 1.1.

Theorem 5.1 (Christodoulou–Klainerman [15]). *Minkowski space is nonlinearly asymptotically stable as a solution of the vacuum Einstein equations (1.2).*

Recall that, in *harmonic gauge*, the vacuum Einstein equations (1.2) take the form of a quasilinear system of wave equations

$$\square_g g_{\mu\nu} = Q_{\mu\nu}(g, \partial g), \quad (5.1)$$

which linearise around Minkowski space to the standard linear wave equation

$$\square_m \psi = 0, \quad (5.2)$$

for each linearised component $\psi = \overset{\circ}{g}_{\mu\nu}$. In $n + 1$ dimensions, solutions decay at the sharp rate

$$|\psi(t, x)| \lesssim \frac{1}{(1+t)^{\frac{n-1}{2}}}.$$

In $3 + 1$ dimensions this rate of $(1+t)^{-1}$, which just fails to be globally integrable, is exactly critical for upgrading to nonlinear stability. Indeed, in $3+1$ dimensions, the trivial solution of (5.1) fails to be nonlinearly stable *for the typical nonlinearity* $Q_{\mu\nu}$. One can only hope for nonlinear stability if there is special structure present in $Q_{\mu\nu}$.

The situation is best exemplified by two model equations

$$\square_m \psi = -(\partial_t \psi)^2, \quad \square_m \psi = -(\partial_t \psi)^2 + |\nabla_x \psi|^2. \quad (5.3)$$

It was shown by John [40] that $\psi \equiv 0$ fails to be nonlinearly stable for the former of (5.3), while for the latter of (5.3) a transformation due to Nirenberg (see [43]) immediately yields global existence. The situation was clarified with the formulation of the *null condition* of Klainerman [44], which identifies a wide class of “good” nonlinearities for which global existence holds.

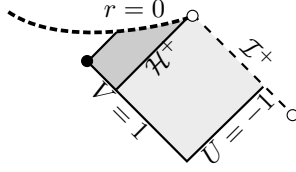


Figure 4: Schwarzschild as a Cauchy development of characteristic data.

One sees the difference between the two nonlinearities of (5.3) by noting the decay rates of derivatives of solutions of (5.2) with respect to the standard double null gauge of Minkowski space

$$|\partial_u \psi(t, x)| \lesssim \frac{1}{1+t}, \quad |\partial_v \psi(t, x)| \lesssim \frac{1}{(1+t)^2}, \quad |\nabla \psi(t, x)| \lesssim \frac{1}{(1+t)^2},$$

expanding the nonlinearities in double null gauge

$$-(\partial_t \psi)^2 = -\frac{1}{4} [(\partial_v \psi)^2 + (\partial_u \psi)^2 + 2\partial_u \psi \partial_v \psi], \quad -(\partial_t \psi)^2 + |\nabla_x \psi|^2 = -\partial_u \psi \partial_v \psi + |\nabla \psi|^2,$$

and noting the presence of the quadratic term in the slowest decaying decay derivative $(\partial_u \psi)^2$ in the former of (5.3), and its absence in the latter.

The null condition of [44] is *not* satisfied by the reduced Einstein equations in harmonic gauge (5.1) (there is, however, a weaker form of the null condition present, as identified and exploited by Lindblad–Rodnianski [51]). The approach taken in [15] was to completely abandon harmonic gauge, and introduce an appropriate geometric formulation, closely related to the double null gauge discussed in Section 3, of the vacuum Einstein equations (1.2), in which an analogue of the null condition is now captured. The double null gauge formulation also captures this null condition.

5.2 The nonlinear stability of Schwarzschild theorem

Before the proof of Theorem 1.1 is outlined, a more precise formulation is given as follows.

In order to define initial data it is convenient to consider a representation of Schwarzschild which is regular beyond the event horizon \mathcal{H}^+ . Accordingly, consider the Kruskal manifold $\mathcal{M}_K = \mathcal{W}_K \times S^2$, where

$$\mathcal{W}_K = \{(U, V) \in \mathbb{R}^2 \mid UV < 1\},$$

equipped with the Kruskal form of the Schwarzschild metric (3.4) (with $r = r(U, V)$ defined implicitly by the relation (3.5)). Note that the future event horizon of Schwarzschild is described in this Kruskal representation by the set $\mathcal{H}^+ = \mathcal{M}_K \cap \{U = 0\} \cap \{V \geq 0\}$. To formulate the theorem consider first the region

$$\mathcal{M}_K \cap \{\delta \geq U \geq -1\} \cap \{1 \leq V < \infty\}, \quad (5.4)$$

for some small $\delta > 0$. See Figure 4.

The above region (5.4) may be viewed as the unique *maximal future Cauchy development* of Schwarzschild characteristic initial data for (1.2) posed on the null hypersurfaces

$$C_{\text{out}} = \{-1\} \times [1, \infty) \times \mathbb{S}^2, \quad \underline{C}_{\text{in}} = [-1, \delta] \times \{1\} \times \mathbb{S}^2. \quad (5.5)$$

See [28, 10] for the general notion of maximal Cauchy development and [61] for the characteristic initial value problem.

Note that $S = \{\delta\} \times \{1\} \times \mathbb{S}^2$ is a *trapped sphere* in Schwarzschild in view of the inequalities $\partial_U r(\delta, 1) < 0$, $\partial_V r(\delta, 1) < 0$. It is the above data which will be perturbed, i.e. characteristic data sets for (3.25)–(3.51) defined on the initial hypersurfaces (5.5) which are assumed suitably close to Schwarzschild initial data will

be considered. In particular, for all data considered, the cone C_{out} will be future complete and asymptotically flat, “terminating” at null infinity \mathcal{I}^+ , while the terminal sphere S of $\underline{C}_{\text{in}}$ will again be trapped. See Chapter 5 of [20] for a more detailed discussion of initial data.

Theorem 1.1 can be more precisely stated as follows.

Theorem 5.2 (The nonlinear asymptotic stability of Schwarzschild in full co-dimension [20]). *For all characteristic initial data prescribed on (5.5), assumed sufficiently close to Schwarzschild data with mass M_{init} and lying on a codimension-3 “submanifold” $\mathfrak{M}_{\text{stable}}$ of the moduli space \mathfrak{M} of initial data, the maximal Cauchy development \mathcal{M} contains a region \mathcal{R} which can be covered by appropriate (teleologically normalised) global double null gauges (3.1) and which*

- (i) *possesses a complete future null infinity \mathcal{I}^+ such that $\mathcal{R} \subset J^-(\mathcal{I}^+)$, and in fact the future boundary of \mathcal{R} in \mathcal{M} is a regular, future affine complete “event horizon” \mathcal{H}^+ . Moreover,*
- (ii) *the metric remains close to the Schwarzschild metric with mass M_{init} in \mathcal{R} (moreover, measured with respect to an energy at the same order as a suitable “initial” energy), and*
- (iii) *asymptotes, inverse polynomially, to a Schwarzschild metric with mass $M_{\text{final}} \approx M_{\text{init}}$ as $u \rightarrow \infty$ and $v \rightarrow \infty$, in particular along \mathcal{I}^+ and \mathcal{H}^+ .*

Note that the celebrated *weak cosmic censorship* conjecture (see [13]) says that for generic asymptotically flat data, the Cauchy evolution possesses a complete future null infinity \mathcal{I}^+ . Statement (i) can thus be thought of as showing “weak cosmic censorship” in a neighbourhood of Schwarzschild, statement (ii) can be thought of as the *orbital stability* of the Schwarzschild exterior, while statement (iii) represents the *asymptotic stability* of the Schwarzschild family—all restricted to the codimension-3 “submanifold” $\mathfrak{M}_{\text{stable}}$ of data, to be discussed further in Section 5.3 below.

For a yet more precise statement of Theorem 1.1, see Theorem 6.1 of [20].

5.3 The 3-parameter families of initial data

Instead of considering the Cauchy evolution of one fixed initial data set, the issue of identifying the codimension 3 “submanifold” is resolved by considering the evolution of an entire 3-parameter family of initial data sets.

The objects which can freely be prescribed as characteristic initial data — i.e., for a given mass $M_{\text{init}} > 0$ and a given small $\varepsilon_0 > 0$, the objects which parameterise the moduli space of initial data in a neighbourhood of Schwarzschild $\mathfrak{M}(M_{\text{init}}, \varepsilon_0)$ — embed naturally into a vector space. One considers three reference fixed mass linearised Kerr sets

$$\mathcal{K}_{-1}, \quad \mathcal{K}_0, \quad \mathcal{K}_1,$$

(which, in linear theory, give rise to the 3 dimensional fixed mass linearised Kerr family of solutions of Definition 4.3). For each appropriate reference initial data set \mathcal{S}_0 , and for parameters $\lambda = (\lambda_{-1}, \lambda_0, \lambda_1) \in \mathbb{R}^3$, one defines

$$\mathcal{S}_0(\lambda) = \mathcal{S}_0 + \sum_{m=-1}^1 \lambda_m \mathcal{K}_m.$$

The moduli space of initial data $\mathfrak{M}(M_{\text{init}}, \varepsilon_0)$ is then decomposed into 3-parameter families

$$\mathcal{L}_{\mathcal{S}_0}^{\varepsilon_0} := \{\mathcal{S}_0(\lambda) : \lambda \in [-c\varepsilon_0, c\varepsilon_0]^3 \subset \mathbb{R}^3\}, \quad (5.6)$$

parameterised by appropriate $\mathcal{S}_0 \in \mathfrak{M}(M_{\text{init}}, c\varepsilon_0)$, where $c > 0$ is a fixed small constant, with the disjointness property

$$\mathcal{S}_0 \neq \mathcal{S}'_0 \implies \mathcal{L}_{\mathcal{S}_0}^{\varepsilon_0} \cap \mathcal{L}_{\mathcal{S}'_0}^{\varepsilon_0} = \emptyset.$$

As \mathcal{S}_0 is varied in a suitable space, these families $\mathcal{L}_{\mathcal{S}_0}^{\varepsilon_0}$ cover $\mathfrak{M}(M_{\text{init}}, \varepsilon_0)$.

Denoting by $(\mathcal{M}(\lambda), g(\lambda))$ the maximal Cauchy development of initial data $\mathcal{S}_0(\lambda)$, the aim is to show that, for each \mathcal{S}_0 , there exists a $\lambda^{\text{final}} \in [-c\varepsilon_0, c\varepsilon_0]^3$ for which $(\mathcal{M}(\lambda^{\text{final}}), g(\lambda^{\text{final}}))$ asymptotes to a Schwarzschild metric as described in the statement of Theorem 5.2. The asymptotically stable “submanifold” will then be defined to be the union

$$\mathfrak{M}_{\text{stable}} = \bigcup_{\mathcal{S}_0 \in \mathfrak{M}_0} \mathcal{S}_0(\lambda^{\text{final}})$$

for the above λ^{final} (which itself depends on \mathcal{S}_0). It is in this sense that the “submanifold” of Theorem 5.2 can be naturally viewed as codimension 3.

See Chapter 5 of [20] for more details regarding the moduli space $\mathfrak{M}(M_{\text{init}}, \varepsilon_0)$ and its decomposition into the 3-parameter families $\mathcal{L}_{\mathcal{S}_0}^{\varepsilon_0}$.

5.4 The logic of the proof

The proof of Theorem 5.2 proceeds by a continuity argument. In order to deal with the aforementioned nonlinear aspects of the problem, several features of the continuity argument are slightly non-standard.

Indeed, consider a given reference seed data set \mathcal{S}_0 and its associated 3-parameter family (5.6). At each stage of the continuity argument, governed by a final retarded time u_f , one considers

- A subset $\mathfrak{R}(u_f) \subset \mathbb{R}^3$ of λ parameter space;
- For each $\lambda \in \mathfrak{R}(u_f)$ a certain *bootstrap region* of the corresponding maximal development $(\mathcal{M}(\lambda), g(\lambda))$;
- Two distinct double null gauges, corresponding to a “near” region and a “far” region, covering the bootstrap region, which are normalised to its future boundaries;
- *Bootstrap assumptions* for the geometric quantities of these double null gauges (for example the Ricci coefficients (3.7)–(3.9) and curvature components (3.10)–(3.12)), on the bootstrap region.

The set of parameters $\mathfrak{R}(u_f)$ is a closed set in \mathbb{R}^3 such that the “total angular momentum” of the corresponding solutions, at retarded time $u = u_f$, is less than or equal to $\varepsilon_0 u_f^{-1}$, with equality holding on the boundary $\partial\mathfrak{R}(u_f)$. This “total angular momentum” is defined as the norm of a vector \mathbf{J} associated to appropriate $\ell = 1$ modes of the curvature component β at retarded time u_f .

The bootstrap assumptions involve comparing the solution to a member of the Schwarzschild family in the Eddington–Finkelstein double null gauge (see Definition 3.3) whose mass M_f is chosen on the basis of the $\ell = 0$ mode of the appropriately weighted curvature component ρ at retarded time u_f . As is usual in a continuity argument, the statement that the bootstrap assumptions can be improved is the main difficulty of the proof. See Section 5.6 below.

The bootstrap region, and the two double null gauges which cover it, are discussed in Section 5.5 below. See Chapter 7 of [20] for more details on the logic of the proof.

5.5 The bootstrap region and the two teleologically normalised gauges

As in [19], in order for the solution to converge to Schwarzschild *in the standard double null gauge* of Example 3.1, it is necessary to normalise the residual double null gauge freedom (see Remark 3.2) *teleologically*. The proof of Theorem 5.2 in fact employs two distinct double null gauges corresponding to:

- A near region, covered by the “ \mathcal{H}^+ gauge”, where the redshift effect, discussed in Section 2.1, is relevant. In the context of the linear wave equation, discussed in Section 2, the redshift effect is a helpful property of Schwarzschild – it has a damping effect on waves. From the backwards viewpoint, however, this redshift effect becomes a *blueshift* and has the opposite effect. If the residual gauge freedom is only normalised in a region far from the event horizon (e.g. if one extended the \mathcal{I}^+ gauge, discussed below, to the entire exterior) then this blueshift would cause certain quantities to *grow exponentially* as they approach the event horizon \mathcal{H}^+ . The \mathcal{H}^+ gauge employed in the proof of Theorem 5.2 is closely related to the teleological gauge employed in [19], discussed in Section 4.5.

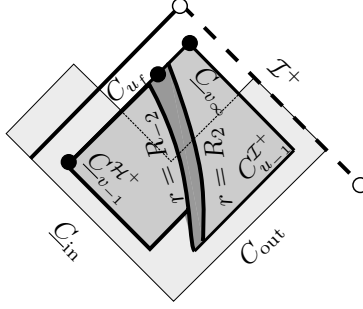


Figure 5: The two teleological double null gauges and the two auxiliary double null gauges near data.

- A far region, covered by the “ \mathcal{I}^+ gauge”, where the null condition, discussed in Section 5.1, is paramount. The essential usefulness of such a normalisation “to \mathcal{I}^+ ” here is that it allows for better control of the decay towards \mathcal{I}^+ , important for capturing the null condition necessary for controlling nonlinear terms error terms (see Section 5.6 below). Though one could have considered the analogue of the normalisations specific to the \mathcal{I}^+ gauge already in [19], it was not necessary in view of the fact that there were no nonlinear terms in the equations to control. It should be remarked again that an additional bonus of this normalisation is that the ultimate \mathcal{I}^+ gauge is *Bondi* (see Section 6.1) and thus the familiar laws of gravitational radiation (see [8, 63] and [15]), along with nonlinear effects such as Christodoulou memory [12], can be immediately understood.

Given a final retarded time u_f and $\lambda \in \mathfrak{R}(u_f)$, the bootstrap region of $(\mathcal{M}(\lambda), g(\lambda))$ is defined to be the intersection of the past of a particular “late” outgoing null cone C_{u_f} and the past of a particular “late” ingoing null cone \underline{C}_{v_∞} , with $v_\infty \rightarrow \infty$ as $u_f \rightarrow \infty$, intersecting at the sphere S_{u_f, v_∞} . In both gauges, defined by double null coordinates $(u_{\mathcal{H}^+}, v_{\mathcal{H}^+})$ and $(u_{\mathcal{I}^+}, v_{\mathcal{I}^+})$ respectively, the final outgoing cone C_{u_f} is a hypersurface of constant $u_{\mathcal{H}^+}$, respectively $u_{\mathcal{I}^+}$, common in the region where the two gauges overlap, anchoring the two gauges together. See Figure 5 for a schematic depiction of the two double null gauges.

The proof of Theorem 5.2 moreover utilises an “initial data region”, covered by a double null gauge in which appropriate local theory (which in fact already requires exploiting the null condition) guarantees that the associated geometric quantities can be made arbitrarily close to their Schwarzschild values by imposing suitable smallness on the initial data. This region is the lighter shaded region in Figure 5.

5.5.1 The normalisation of the \mathcal{H}^+ and \mathcal{I}^+ gauges

The \mathcal{H}^+ gauge is normalised on the “late” outgoing null cone C_{u_f} and an initial ingoing cone $\underline{C}_{v_{-1}}^{\mathcal{H}^+}$ defined by $v_{\mathcal{H}^+} = v_{-1}$. This initial cone does not coincide with the initial data cone $\underline{C}_{\text{in}}$ but remains within a fixed distance from $\underline{C}_{\text{in}}$ independently of u_f . The gauge will only be considered in a region $r \leq R_2$, where r is a function of $(u_{\mathcal{H}^+}, v_{\mathcal{H}^+})$.

The \mathcal{I}^+ gauge admits the cone \underline{C}_{v_∞} as a $v_{\mathcal{I}^+} = v_\infty$ hypersurface, and the geometry of the cones is normalised on the final ingoing cone \underline{C}_{v_∞} and the “initial” outgoing cone $C_{u_{-1}}^{\mathcal{I}^+}$ defined by $u_{\mathcal{I}^+} = u_{-1}$. As before, this initial cone does not coincide with the initial data cone C_{out} but remains within a fixed distance from C_{out} independently of u_f . The gauge will only be considered in a region $r \geq R_{-2}$, with $R_{-2} < R_2$, where r is a function of $(u_{\mathcal{I}^+}, v_{\mathcal{I}^+})$. The two r functions are close and the gauges thus have a nontrivial overlap region (the darker shaded region in Figure 5).

The normalisations are determined by a series of requirements on the spheres $S_{u_f, v_{-1}}$ and $S_{u_f, v(R, u_f)}$, for an $R_{-2} < R < R_2$, and on the cones $C_{u_f}, \underline{C}_{v_{-1}}^{\mathcal{H}^+}$ in the case of the \mathcal{H}^+ gauge, and on the sphere S_{u_f, v_∞} and the cones $C_{u_{-1}}^{\mathcal{I}^+}, \underline{C}_{v_f}$ in the case of the \mathcal{I}^+ gauge. For example, part of the defining properties of the \mathcal{I}^+

gauge are the requirements

$$\Omega \text{tr} \chi - (\Omega \text{tr} \chi)_\circ = 0, \quad \Omega^{-1} \text{tr} \underline{\chi} - (\Omega^{-1} \text{tr} \underline{\chi})_\circ = 0 \text{ on } S_{u_f, v_\infty} \quad (5.7)$$

and

$$\mu_{\ell \geq 1} = 0 \text{ on } \underline{C}_{v_\infty}. \quad (5.8)$$

Here $(\Omega \text{tr} \chi)_\circ$, $(\Omega^{-1} \text{tr} \underline{\chi})_\circ$ denote the Schwarzschild quantities of Example 3.3, and the Ricci coefficient μ denotes the mass-aspect function, defined by

$$\mu = \text{div} \eta + \rho - \frac{1}{2}(\hat{\chi}, \hat{\chi}).$$

See the common proof of Proposition 9.2.2–9.2.4 of [19] for the motivation for (5.7)–(5.8). These normalisations ensure that as $(u_f, v_\infty) \rightarrow (\infty, \infty)$, the normalisation of the \mathcal{I}^+ gauge becomes Bondi, and moreover, we have vanishing of the quantity $\Sigma_+ = \lim_{u_{\mathcal{I}^+} \rightarrow \infty} \lim_{v_{\mathcal{I}^+} \rightarrow \infty} r^2 \hat{\chi}(u, v) = 0$ (see also Section 6.1 below). In this limit the bootstrap region becomes the black hole exterior.

Similar conditions to (5.7)–(5.8) appeared as the relations determining the spheres foliating the spacelike hypersurface Σ_* of [47].

Note again that the two gauge normalisations are non-trivial at the linearised level and differ in their overlap already in linear theory. See Chapter 2 of [20] for more details on the normalisations of the \mathcal{H}^+ and \mathcal{I}^+ gauges.

Part of the proof of Theorem 5.2 involves the construction of the \mathcal{H}^+ and \mathcal{I}^+ gauges achieving these normalisations. The existence is shown using an implicit function theorem style argument. See Section 16.1 of [20] for more details.

5.5.2 Diffeomorphism functions relating gauges and boundedness of initial norms

Recall the above setting of Section 5.5.1, and recall in particular that the “initial hypersurface” $C_{u_{-1}}^{\mathcal{I}^+}$ of the \mathcal{I}^+ gauge does not coincide with the hypersurface C_{out} , but lies within a fixed distance from it. Similarly for the hypersurface $\underline{C}_{v_{-1}}^{\mathcal{H}^+}$ of the \mathcal{H}^+ gauge. As in [19], the starting point of the analysis is the quantities α and $\underline{\alpha}$ (see Section 5.6 below). As these quantities are associated to the future normalised \mathcal{I}^+ and \mathcal{H}^+ gauges (and are no longer gauge invariant but only “almost gauge invariant”, or gauge invariant to linear order), the “initial norms” on the hypersurfaces $C_{u_{-1}}^{\mathcal{I}^+}$ and $\underline{C}_{v_{-1}}^{\mathcal{H}^+}$ are not equal to the corresponding norms of the α and $\underline{\alpha}$ of the initial gauge (on which the smallness assumption is made), but are equal only up to nonlinear terms. These nonlinear terms involve the diffeomorphism functions relating the corresponding gauges to the initial gauge, which thus have also to be controlled as part of the proof of Theorem 5.2 (see also the underlined statement in Theorem 4.4 for the analogue of such control in linear theory).

The general idea for estimating the diffeomorphisms connecting the various gauges is to use relations expressing the difference of curvature or Ricci coefficients in the two gauges, in which derivatives of the gauge functions appear. For instance, one can write schematically the relation for the difference of the curvature component β expressed in two gauges

$$\Omega \beta - \widetilde{\Omega} \beta = \frac{6M}{r^3} \left(1 - \frac{2M}{r}\right) \nabla f^3 + \dots,$$

where nonlinear terms are omitted and f^3 here denotes one component of the diffeomorphism connecting the gauges (see Chapter 4 of [20] for a complete list of such relations, and compare with the pure gauge solutions of the linearised equations of Definition 4.2). From the above, estimates on curvature components like $\Omega \beta$ and $\widetilde{\Omega} \beta$, to be discussed below, lead to estimates on f^3 . It is necessary to exploit a form of null condition (see Section 5.1) in the omitted nonlinear terms when estimating the diffeomorphisms relating the \mathcal{I}^+ gauge to the initial gauge. See Chapter 10 of [20] where the procedure for estimating these diffeomorphisms, along with the “initial norms” of $\alpha_{\mathcal{I}^+}$ and $\alpha_{\mathcal{H}^+}$, is implemented in full.

5.6 The main estimates

As in [19], the starting point of the analysis is the curvature components α and $\underline{\alpha}$ (see (3.10)). The quantity α now satisfies wave equation of the form

$$-\Omega\check{\nabla}_4\Omega\check{\nabla}_3(r\Omega^2\alpha) + \Omega^2\check{\Delta}(r\Omega^2\alpha) - \frac{4}{r}\left(1 - \frac{3M}{r}\right)\Omega\check{\nabla}_3(r\Omega^2\alpha) - \frac{2\Omega^2}{r^2}\left(1 + \frac{3M}{r}\right)r\Omega^2\alpha = \mathcal{E}[\alpha], \quad (5.9)$$

where $r = r(u, v)$ is again defined implicitly via the relation (3.3) (but no longer has the interpretation as the area radius of the spheres of the double null foliations). In fact, since there are two separate gauges — the \mathcal{I}^+ gauge and the \mathcal{H}^+ gauge — there is a separate α associated to each, denoted $\alpha_{\mathcal{I}^+}$ and $\alpha_{\mathcal{H}^+}$ respectively. Each satisfy equation (5.9) with respect to their corresponding gauges. Equation (5.9) is analogous to the linear Teukolsky equation (4.32), but now couples to the other geometric quantities of the system via the term $\mathcal{E}[\alpha]$, which can be written schematically as

$$\mathcal{E}[\alpha] = \Omega^2 \sum_{p_1+p_2 \geq 6} \sum_{\substack{k_1 \leq 1 \\ k_2 \geq 2}} r^{-p_1} \cdot (\mathfrak{D}^{k_1} \Phi_{p_2})^{k_2}, \quad (5.10)$$

where Φ_p is a schematic notation encompassing both Ricci coefficients Γ_p and curvature components \mathcal{R}_p , but now for *differences* of quantities from their Schwarzschild values (defined with respect to each double null gauge via the Schwarzschild expressions of Example 3.3). The p indices are used to encode appropriate r behaviour of the various geometric quantities. See Chapter 3 of [20] for a precise definition of this schematic notation. The error $\mathcal{E}[\alpha]$ is quadratic in such differences (encoded in (5.10) by the fact that $k_2 \geq 2$) and thus can be viewed as a nonlinear error term. The fact that $p_1 + p_2 \geq 6$ in each of these nonlinear error terms encodes the fact that $\mathcal{E}[\alpha]$ decays in r (in an appropriate sense) at the fast rate of r^{-6} , thus exhibiting an appropriate version of the null condition discussed in Section 5.1. (The fact that $k_1 \leq 1$ in (5.10) encodes the fact that at most one derivative of the Ricci coefficients or curvature components can appear in each term.)

As in Section 4.4, defining

$$P = -\frac{1}{2r^3\Omega}\check{\nabla}_3(r^2\Omega^{-1}\check{\nabla}_3(r\Omega^2\alpha)),$$

one sees that P satisfies a nonlinear analogue of the Regge–Wheeler equation (4.40), namely

$$-\Omega\check{\nabla}_4\Omega\check{\nabla}_3(r^5P) + \left(1 - \frac{2M}{r}\right)\check{\Delta}(r^5P) - \left(\frac{4}{r^2} - \frac{6M}{r^3}\right)\left(1 - \frac{2M}{r}\right)P = \mathcal{E}[P], \quad (5.11)$$

where $\mathcal{E}[P]$ takes the schematic form

$$\mathcal{E}[P] = \Omega^2 \sum_{p_1+p_2 \geq 2} \sum_{\substack{k_1 \leq 3 \\ k_2 \geq 2}} r^{-p_1} \cdot (\mathfrak{D}^{k_1} \Phi_{p_2})^{k_2}. \quad (5.12)$$

Again, there is a P associated to each of the \mathcal{I}^+ and \mathcal{H}^+ gauges, denoted $P_{\mathcal{I}^+}$ and $P_{\mathcal{H}^+}$ respectively, neither of which are defined on the entire bootstrap region, but only on the regions covered by the \mathcal{I}^+ and \mathcal{H}^+ gauges respectively (see Section 5.5). The analysis for \check{P} carried out in [19], described in the context of the wave equation in Section 2, is then repeated to obtain decay estimates for P , accounting for the following differences:

- The “initial norms” of $P_{\mathcal{I}^+}$ and $P_{\mathcal{H}^+}$, defined on the hypersurfaces $\underline{C}_{u_{-1}}^{\mathcal{I}^+}$ and $\underline{C}_{v_{-1}}^{\mathcal{H}^+}$, are not equal to the corresponding norms of the P associated to the initial gauge (but are only equal to linear order). In order to relate these norms to the smallness parameter ε_0 , the control of the diffeomorphisms discussed in Section 5.5.2 is exploited.

- There is no “global” P defined on the entire bootstrap region. Accordingly, $P_{\mathcal{I}^+}$ is estimated to the right of an appropriate timelike hypersurface \mathcal{B} , and $P_{\mathcal{H}^+}$ is estimated to the left of \mathcal{B} . In view of the fact that P is “almost gauge invariant”, the corresponding boundary terms on \mathcal{B} cancel to linear order. In order to control the nonlinear terms, the procedure outlined in Section 5.5.2 is repeated to control the diffeomorphisms relating the \mathcal{I}^+ and \mathcal{H}^+ gauges in the region on which they overlap. The timelike hypersurface \mathcal{B} is chosen by a suitable averaging procedure, as in [25], and thus depends on both the solution, and the bootstrap time u_f , in a non-continuous manner in general.
- There are nonlinear error terms on the right hand side of (5.11) to estimate. In the context of energy-type estimates (as discussed in Section 2), after commutation $N - 3$ times by suitable operators \mathfrak{D} , the error $\mathcal{E}[P]$ (see (5.12)) produces terms which are cubic and higher, e.g. terms of the form

$$\mathfrak{D}^{N-2}P \cdot \mathfrak{D}^N\Phi \cdot \Phi \tag{5.13}$$

in schematic notation, which must be integrated over spacetime with weights. The highest order terms $\mathfrak{D}^{N-2}P$ and $\mathfrak{D}^N\Phi$ (an example of the latter are highest order commuted curvature terms like $\mathfrak{D}^N\alpha$), must typically be estimated in the energy norm, whereas lower order terms Φ in (5.13) must be taken in a higher L^p norm, say L^∞ . The most difficult regions for controlling these non-linear terms are near null infinity \mathcal{I}^+ and near the Schwarzschild photon sphere $r = 3M$. For it is in these two regions where it cannot be ensured that the spacetime integral of the highest order terms is controlled by the natural (weighted) integrated local energy decay estimates (recall the discussion in Section 2.5). Thus, in general, to obtain spacetime integrability of the terms (5.13) one must exploit some sort of time-decay for the lower order terms.

- **Error terms near null infinity \mathcal{I}^+ :** In this region the null condition, described in Section 5.1, is relevant. The null condition is exhibited in the nonlinear error term $\mathcal{E}[P]$ in the fact that $p_1 + p_2 \geq 2$ in each term in (5.12), encoding decay in r (in an appropriate sense) of $\mathcal{E}[P]$ at the fast rate of r^{-2} .
- **Error terms around the Schwarzschild photon sphere $r = 3M$:** When terms of the form (5.13) are integrated over spacetime, they can typically be controlled using boundedness of the lower order quantity Φ , and integrated decay estimates (see Section 2) for the higher order quantities

$$\int \int |\mathfrak{D}^{N-2}P \cdot \mathfrak{D}^N\Phi \cdot \Phi| dx dt \lesssim \sup |\Phi| \int \int |\mathfrak{D}^{N-2}P|^2 + |\mathfrak{D}^N\Phi|^2 dx dt.$$

Such a scheme is problematic, at top order, around $r = 3M$ however, in view of the degeneration of the integrated decay estimates due to the presence of trapped null geodesics. See Proposition 2.9. Instead, one must exploit the boundedness of the energy of the two higher order terms, and *decay* of the lower order term

$$\int \int |\mathfrak{D}^{N-2}P \cdot \mathfrak{D}^N\Phi \cdot \Phi| dx dt \lesssim \int \sup_x |\Phi| dt \sup_t \int |\mathfrak{D}^{N-2}P|^2 + |\mathfrak{D}^N\Phi|^2 dx.$$

It would seem that decay strictly faster than t^{-1} is necessary for the lower term in order to make the above integral finite. In fact, such faster decay is only required in an averaged sense, of the form

$$\int_t^\infty |\Phi|^2 dt' \lesssim \frac{1}{t^{1+\delta}}.$$

See Section 11.7.1 of [20] for more details.

The analysis of α and $\underline{\alpha}$ described above is completed in detail in Chapters 11–13 of [20]. Once α and $\underline{\alpha}$ are viewed as given, the remainder of the system (3.25)–(3.51) can again be viewed as a system of transport and elliptic equation, which are now nonlinear. They admit a hierarchical structure, as discussed in Section 4.5, which now only effectively decouples the system *to linear order*. The remainder of the geometric

quantities are estimated by exploiting gauge conditions and integrating this system of transport equations backwards in this hierarchical manner in each of the \mathcal{I}^+ and \mathcal{H}^+ gauges. See Chapter 14 and Chapter 15 of [20] respectively for more details.

5.7 The completion of the continuity argument

Recall the logic of the proof, described in Section 5.4. Once the bootstrap assumptions are improved, one aims to show that, for some fixed u_f^0 , the set $\mathfrak{B} \subset [u_f^0, \infty)$ of “allowed” final retarded times u_f (i.e. the set \mathfrak{B} of u_f such that an appropriate region $\mathfrak{R}(u_f)$ of λ parameter space exists, the \mathcal{I}^+ and \mathcal{H}^+ gauges described in Section 5.5 can be constructed for each corresponding solution, and such that the bootstrap assumptions indeed hold for each solution) is a non-empty, open and closed subset of $[u_f^0, \infty)$, and thus $\mathfrak{B} = [u_f^0, \infty)$.

The standard structure for such an argument is to appeal to Cauchy stability to obtain that $u_f^0 \in \mathfrak{B}$ and then to the improvement of the bootstrap assumptions, together with an appropriate local existence theorem, to show that one can extend the bootstrap region. The present setup, however, requires two additional slightly non-standard features, related to the finite codimensionality nature of the result and the teleological nature of the gauge:

- **Finite codimensionality:** Recall that there is now a varying set of parameters $\mathfrak{R}(u_f)$. The definition of the sets $\mathfrak{R}(u_f)$ and appropriate estimates for the geometric quantities result in the monotonicity statement

$$u'_f > u_f \quad \implies \quad \mathfrak{R}(u'_f) \subset \mathfrak{R}(u_f), \quad \mathfrak{R}(u'_f) \cap \partial\mathfrak{R}(u_f) = \emptyset. \quad (5.14)$$

By a strengthening of Cauchy stability type arguments, the original region $\mathfrak{R}(u_f^0)$ can be seen to be a closed disc and the map $\mathbf{J}_0 : \mathfrak{R}(u_f^0) \rightarrow B$ defined by $\mathbf{J}_0(\lambda) := (\lambda, u_f^0)$, mapping to an appropriate closed ball $B \subset \mathbb{R}^3$, can be seen to have degree 1 on $\partial\mathfrak{R}(u_f^0)$. A topological argument applied to an appropriately defined map \mathbf{J}_{u_f} can then be used to show that $\mathfrak{R}(u_f)$ indeed remains non-empty for all $u_f > u_f^0$. See Section 16.2 of [20] for more details.

- **Teleological normalisation of the gauge:** Enlarging the bootstrap region requires an appeal to an iteration argument around the analogous linearised construction in order to select the new “final” sphere $S_{u'_f, v'_\infty}$ of an enlarged region and achieve the gauge normalisations such as (5.7)–(5.8) described in Section 5.5. By continuity of the gauge renormalisation procedure, the bootstrap assumptions remain improved in the enlarged region, provided the region is enlarged by a sufficiently small amount.

Once it has been established that $\mathfrak{B} = [u_f^0, \infty)$, one obtains in view of (5.14) that there exists $\lambda^{\text{final}} = (\lambda_{-1}^{\text{final}}, \lambda_0^{\text{final}}, \lambda_1^{\text{final}})$, such that $\lambda^{\text{final}} \in \mathfrak{R}(u_f)$ for all $u_f \geq u_f^0$, and a solution $(\mathcal{M}, g) := (\mathcal{M}(\lambda^{\text{final}}), g(\lambda^{\text{final}}))$ generated by data $\mathcal{S} := \mathcal{S}_0(\lambda^{\text{final}})$, with an M_f tending to the final Schwarzschild mass M_{final} and with “final total angular momentum” zero. It is therefore this collapsing of the 3-parameter family (5.6) which leads to the codimension-3 statement of Theorem 5.2.

6 Conclusions and outlook

The proof of Theorem 1.1 immediately yields conclusions concerning the familiar laws of gravitational radiation (see [8, 63] and [15]), and nonlinear effects such as Christodoulou memory [12], along with properties of the event horizon \mathcal{H}^+ . These conclusions are described in Section 6.1.

Though the codimension-3 “submanifold” of Theorem 1.1 is only characterised teleologically (cf. the discussion at the beginning of Section 5), there are infinite codimension subfamilies which can be characterised explicitly. Such a family is identified in a corollary of Theorem 1.1, stated in Section 6.2.

The remainder of this section concerns three conjectures, concerning the nonlinear stability of the Kerr family in the full subextremal range, a discussion of extremal black holes and the Aretakis instability, and the black hole interiors of the solutions of Theorem 1.1, in Sections 6.3, 6.4, and 6.5 respectively.

6.1 Properties of \mathcal{I}^+ and \mathcal{H}^+

For the solutions of Theorem 1.1, statements about the properties of null infinity \mathcal{I}^+ , as well as the existence and regularity of the event horizon \mathcal{H}^+ , are easily obtained a posteriori as a result of the proof.

Consider a given solution of Theorem 1.1 and recall that (see Section 5.5), for each bootstrap time u_f , there is a bootstrap region which is covered by appropriate \mathcal{I}^+ and \mathcal{H}^+ gauges. One obtains the existence of limiting \mathcal{I}^+ and \mathcal{H}^+ gauges, satisfying limiting analogues of the gauge conditions defining \mathcal{I}^+ and \mathcal{H}^+ gauges, by an Arzela–Ascoli argument. By taking the limit of the estimates obtained in the bootstrap regions, one moreover has good estimates for the geometric quantities of these gauges.

The limiting \mathcal{I}^+ gauge is *Bondi*, meaning that

- The spheres of the double null foliation become round at infinity:

$$\lim_{v \rightarrow \infty} r^{-2} \not{g}_{AB}(u, v, \theta^1, \theta^2) = \gamma_{AB}(\theta^1, \theta^2),$$

for all u, θ^1, θ^2 , where γ denotes the unit round metric on S^2 ;

- The foliation by the level hypersurfaces of u becomes affine at \mathcal{I}^+ :

$$\lim_{v \rightarrow \infty} \Omega(u, v, \theta^1, \theta^2) = 1,$$

for all u, θ^1, θ^2 .

Since this limiting \mathcal{I}^+ gauge is defined for all $u \in [0, \infty)$, it immediately follows that future null infinity \mathcal{I}^+ is complete in the sense of Christodoulou [13].

The estimates of the limiting \mathcal{I}^+ gauge allow the existence of appropriate limiting quantities, regarded as tensor fields on $[0, \infty) \times S^2$, to be concluded. For example, one has the existence of the limits

$$\Xi_{AB}(u, \theta) = \lim_{v \rightarrow \infty} r^{-1} \hat{\chi}_{AB}(u, v, \theta), \quad \Sigma_{AB}(u, \theta) = \lim_{v \rightarrow \infty} \hat{\chi}_{AB}(u, v, \theta),$$

and

$$M(u) = \lim_{v \rightarrow \infty} \sqrt{\frac{\text{Area}(S_{u,v})}{16\pi}} \left(1 + \frac{1}{16\pi} \int_{S_{u,v}} \text{tr} \chi \text{tr} \underline{\chi} dA \right).$$

The quantity Ξ is known as the *Bondi news function*, and the function M is known as the *Bondi mass* (defined as the limit of *Hawking masses*). These quantities moreover satisfy familiar laws of gravitation such as

$$\frac{\partial \Sigma}{\partial u} = -\Xi,$$

and the *Bondi mass loss law*

$$\frac{d}{du} M(u) = -\frac{1}{8\pi} \int_{S^2} |\Xi(u, \theta)|^2 d\mu_\gamma.$$

Moreover, the quantity Σ has vanishing future limit

$$\Sigma^+(\theta) := \lim_{u \rightarrow \infty} \Sigma(u, \theta) = 0. \tag{6.1}$$

Note that the quantity Σ features in the celebrated Christodoulou memory effect [12] in which $\Sigma^+(\theta) - \Sigma(0, \theta)$ is related to the total displacement of test masses in gravitational wave experiments. The normalisation (6.1) is a necessary consequence of the requirement to obtain decay for all quantities (in particular $\hat{\chi}$) at constant r . One moreover has

$$M_{\text{final}} = \lim_{u \rightarrow \infty} M(u),$$

i.e. the *final Bondi mass* coincides with the final Schwarzschild parameter.

The uniform estimates in the asymptotic \mathcal{H}^+ normalised gauge, together with the presence of a trapped surface in the initial data which provides a barrier, allow one to extract a limiting, regular hypersurface \mathcal{H}^+ .

Another appeal to local existence of the characteristic initial value problem ensures that \mathcal{H}^+ is indeed in the maximal development (\mathcal{M}, g) (and thus also a neighbourhood of \mathcal{I}^+). It is clear moreover that \mathcal{H}^+ is the future boundary of $J^-(\mathcal{I}^+)$, when the latter is interpreted in the obvious way, i.e. \mathcal{H}^+ is indeed the event horizon of the black hole region of (\mathcal{M}, g) . The future completeness of \mathcal{H}^+ , together with decay along \mathcal{H}^+ for various quantities, follows directly from the estimates.

See Section 7.7 and Chapter 17 of [20] for more details on the properties of \mathcal{I}^+ and \mathcal{H}^+ .

6.2 Axisymmetric solutions with vanishing angular momentum

It is well known that under the assumption of axisymmetry, vacuum solutions cannot radiate angular momentum to null infinity. This fact can be shown using the conservation of the Komar angular momentum $\mathcal{J}(S)$ associated to a 2-surface S (see [67]), and leads easily to the following corollary of Theorem 1.1.

Corollary 6.1 (Nonlinear stability of Schwarzschild under axisymmetric perturbations with vanishing initial angular momentum). *All characteristic initial data prescribed on (5.5), assumed sufficiently close to Schwarzschild data with mass M_{init} , which are moreover axisymmetric and have vanishing Komar angular momentum, are contained in the codimension-3 “submanifold” $\mathfrak{M}_{\text{stable}}$ of Theorem 5.2. Thus, consequences (i), (ii) and (iii) apply to such data.*

Even though the full codimension-3 “submanifold” $\mathfrak{M}_{\text{stable}}$ of Theorem 5.2 can only be characterised teleologically, Corollary 6.1 identifies a further *infinite*-codimension submanifold which can indeed be explicitly identified examining only initial data, namely axisymmetric solutions with vanishing Komar angular momentum.

6.3 The nonlinear stability of the Kerr exterior

For completeness, a statement of the full non-linear stability of the Kerr exterior is given. To compare with Theorem 5.2, the problem is stated in double null gauge. (Recall that the paper [59] exhibits the Kerr metric itself in precisely such a gauge (for the full subextremal range $|a| < M$.) Fixing parameters, we consider then the subregion of Kerr given as the maximal Cauchy development of the union of two null hypersurfaces $\underline{C}_{\text{in}} \cup C_{\text{out}}$ of the double null gauge, where as before $\underline{C}_{\text{in}}$ crosses the event horizon, while C_{out} is future complete and terminates at null infinity.

Conjecture 6.2 (Nonlinear stability of the Kerr exterior). *For all characteristic data prescribed as above, assumed sufficiently close to Kerr with parameters $|a_{\text{init}}| < M_{\text{init}}$, the maximal Cauchy development \mathcal{M} contains a region \mathcal{R} which can be covered by appropriate global double null foliations (3.1) and which (i) possesses a complete future null infinity \mathcal{I}^+ such that $\mathcal{R} \subset J^-(\mathcal{I}^+)$, and in fact the future boundary of \mathcal{R} in \mathcal{M} is a regular future affine complete “event horizon” \mathcal{H}^+ . Moreover (ii) the metric remains close to Kerr in \mathcal{R} and (iii) asymptotes, inverse polynomially, to a Kerr metric with parameters $|a_{\text{final}}| < M_{\text{final}}$ where $a_{\text{final}} \approx a_{\text{init}}$, $M_{\text{final}} \approx M_{\text{init}}$, as $u \rightarrow \infty$ and $v \rightarrow \infty$, in particular along \mathcal{I}^+ and \mathcal{H}^+ .*

Moreover, for any given $0 < |a_{\text{final}}| < M_{\text{final}}$, the set of initial data above attaining these final parameters is codimension-2 in the space of all data, the set of initial data attaining $a_{\text{final}} = 0$ for some M_{final} is codimension-3, and the set of initial data attaining $a_{\text{final}} = 0$ and a fixed M_{final} is codimension-4. In particular, for generic initial data, $a_{\text{final}} \neq 0$, while the set of solutions $a_{\text{final}} = 0$ corresponds precisely to the solutions constructed in Theorem 5.2.

The difference in dimensionality in the $a_{\text{final}} = 0$ case arises from the enhanced symmetry of Schwarzschild in comparison to Kerr.

In view of the recent [17, 62], the path is now open to obtaining Conjecture 6.2 following the approach of [20], although, at a technical level, the Kerr case introduces new complications related to the necessity of applying frequency localisation to deal with the issues related to trapping. In this sense, one of the appealing features of having a complete, self-contained physical space treatment of the Schwarzschild case as described here is that that one may understand the essence of the above conjecture without this additional,

largely technical, complication. For further remarks on the Kerr problem, see recent work of Klainerman–Szeftel [48, 49] and references therein.

One might also consider a restricted version of Conjecture 6.2 in which $|a_{\text{init}}| \ll M_{\text{init}}$ is small, in which case aspects of the Schwarzschild theory can be perturbed. This is work in progress of several groups, including recent and forthcoming work of Klainerman–Szeftel, Giorgi–Klainerman–Szeftel, Shen [33], [50].

6.4 Extremality and the Aretakis instability

Note that the extremal case $|a_{\text{init}}| = M_{\text{init}}$ is excluded from Conjecture 6.2. In fact, a basic understanding of solutions of the linear wave equation on a fixed extremal Kerr background (cf. the discussion of the wave equation on Schwarzschild in Section 2) is still lacking. It is known, however, that all stationary extremal black holes are subject—at the very least—to the Aretakis instability [4] along their event horizon, according to which higher order translation invariant derivatives of solutions to the wave equation generically blow up polynomially. It is interesting to understand whether the most basic geometric features of these black hole spacetimes can still be nonlinearly stable despite this higher order instability phenomenon associated to their event horizons, or, rather, whether this growing “hair” leads at the nonlinear level to some worse type of blowup, for instance the formation of so-called “naked singularities”, resulting in a future incomplete \mathcal{I}^+ (i.e. already violating the analogue of statement (i) of Theorem 5.2). So far, this question has only been probed numerically for toy models under spherical symmetry [56].

In order to disentangle the Aretakis instability from other difficulties associated to extremal Kerr, it is natural to first consider the electrovacuum Reissner–Nordström metrics (see for instance [67]), a spherically symmetric family of solutions to the Einstein–Maxwell system with parameters Q and M . (Note that this family contains the Schwarzschild family as the subfamily $Q = 0$.) One expects that the analogue of Theorem 5.2 for the sub-extremal case $0 \leq Q < M$ of Reissner–Nordström is a more or less straightforward adaptation of the results of the present paper, in view of the recent [31] and [32], where a linear stability proof is carried out explicitly for the subextremal Reissner–Nordström family, adapting the methods of [19] and [47]. The interesting case to consider further is thus the extremal case $Q = M$.

To set up the problem, fix null hypersurfaces $\underline{C}_{\text{in}} \cup C_{\text{out}}$ in background extremal Reissner–Nordström with parameters $M_{\text{init}} = Q_{\text{init}}$, analogous to (5.5), where the terminal sphere of $\underline{C}_{\text{in}}$ lies in the black hole interior. (Note that, in contrast to the Schwarzschild case, this terminal sphere is no longer trapped.) Consider now the moduli space \mathfrak{M} of nearby data defined on $\underline{C}_{\text{in}} \cup C_{\text{out}}$, suitably normalised. Note that we may identify the following families of initial data corresponding to explicit solutions:

- (a) a 1-parameter family corresponding to extremal Reissner–Nordström metrics with charge $Q = M$;
- (b) a 1-parameter family corresponding to Reissner–Nordström metrics with fixed $M = M_{\text{init}}$, parametrised by Q ,
- (c) a 3-parameter family corresponding to extremal Kerr–Newman metrics (see [55]) with charge Q_{init} .

Note that (b) contains both subextremal $Q < M_{\text{init}}$ and superextremal $Q > M_{\text{init}}$ Reissner–Nordström data on $\underline{C}_{\text{in}} \cup C_{\text{out}}$. The latter lead to spacetimes such that $\underline{C}_{\text{in}} \subset J^-(\mathcal{I}^+)$, i.e. spacetimes that fail to form black holes.

For the extremal Reissner–Nordström family (a) itself, then, in view of the above, the best one can hope is for the existence of a codimension-4 asymptotically stable “submanifold” $\mathfrak{M}_{\text{stable}} \subset \mathfrak{M}$, where moreover the asymptotic stability statement is suitably relaxed along \mathcal{H}^+ (compared to that of Theorem 5.2), so as to accommodate the growing horizon “hair” associated to the Aretakis instability. This suggests the following:

Conjecture 6.3 (Asymptotic stability of extremal Reissner–Nordström but with growing horizon “hair”). *For all characteristic initial data for the Einstein–Maxwell system prescribed on (5.5), assumed sufficiently close to extremal Reissner–Nordström data with mass M_{init} and $Q_{\text{init}} = M_{\text{init}}$ and lying on a codimension-4 “submanifold” $\mathfrak{M}_{\text{stable}}$ of the moduli space \mathfrak{M} of initial data, the maximal Cauchy development \mathcal{M} contains a region \mathcal{R} which can be covered by appropriate (teleologically normalised) global double null gauges (3.1) and where the analogues of (i), (ii) and (iii) of Theorem 5.2 are satisfied with an extremal Reissner–Nordström*

metric with parameters $M_{\text{final}} = Q_{\text{final}}$ in the place of Schwarzschild. Along \mathcal{H}^+ , however, one has decay to extremal Reissner–Nordström only in a weaker sense, in particular, for generic data lying on $\mathfrak{M}_{\text{stable}}$, suitable higher order quantities in the arising solution blow up polynomially along \mathcal{H}^+ (growing horizon “hair”).

Given a positive resolution of the above, one would moreover expect that the “submanifold” $\mathfrak{M}_{\text{stable}}$ itself lies on a larger codimension-1 submanifold $\mathfrak{M}'_{\text{stable}}$ of \mathfrak{M} consisting of data leading to solutions asymptoting to a very slowly rotating extremal Kerr–Newman, again with growing horizon hair. Moreover, one could hope to prove that this larger submanifold $\mathfrak{M}'_{\text{stable}}$ delimits the boundary signifying a phase transition between two very different open regions of moduli space \mathfrak{M} : (1) the set of data leading to spacetimes failing to collapse (i.e. those for which $C_{\text{in}} \subset J^-(\mathcal{I}^+)$) and (2) the set of data leading to a black hole exterior settling down to a very slowly rotating subextremal Kerr–Newman spacetime. (Of course, one can already conjecture the analogue of Conjecture 6.3 for extremal Kerr as a family of the Einstein vacuum equations; it is emphasised, however, that the dynamics near this phase transition in that case may be considerably more complicated!)

In order to prove Conjecture 6.3, one must confront a fundamental new difficulty compared to the present work: In the extremal case, the stabilising mechanism of the redshift effect (see Section 2.1), exploited heavily here, degenerates at \mathcal{H}^+ . Moreover, in view of the expected growing horizon hair, it would seem that in order to control the nonlinearities, one must identify and exploit a suitable null condition, not just near null infinity \mathcal{I}^+ as before (cf. Section 5.1), but now also in the region near the event horizon \mathcal{H}^+ . See the recent [2] where such structure is indeed exploited to show global stability results on a fixed extremal Reissner–Nordström background for a nonlinear scalar wave equation whose nonlinearities satisfy the null condition. We hope that the work [20] described in the present lectures, with its set-up for proving finite-codimensional stability statements and with one of its teleological gauges normalised at the event horizon \mathcal{H}^+ , may provide a suitable general framework to try to address Conjecture 6.3.

6.5 Strong cosmic censorship and the black hole interior

Returning to the subextremal case, Conjecture 6.2 can be applied together with the following theorem to obtain the C^0 stability of the Kerr Cauchy horizon:

Theorem 6.4 (C^0 stability of the Kerr Cauchy horizon [21]). *Consider general characteristic initial data for the Einstein vacuum equations on $\mathcal{H}^+ \cup \underline{C}_{\text{in}}$ such that \mathcal{H}^+ is future complete and the data along \mathcal{H}^+ approach that of a sub-extremal rotating Kerr solution (with $0 < |a| < M$) along its event horizon at a suitable inverse polynomial rate. Then restricting to a sufficiently short $\underline{C}_{\text{in}}$, the maximal Cauchy development can be covered by a global double null foliation and can be extended continuously beyond a non-trivial Cauchy horizon \mathcal{CH}^+ .*

In particular, for initial data as in Conjecture 6.2, then as long as $a_{\text{final}} \neq 0$ (which would be true generically!), it would follow from the conjecture and the above paragraph that the maximal Cauchy development is extendible beyond a non-trivial Cauchy horizon located in the black hole interior. In particular, the C^0 -formulation of strong cosmic censorship (see [13]) is false.

In fact, if one considers now two-ended Kerr initial data Σ as depicted in Figure 6, then a further extension of Theorem 6.4, see the upcoming [22], implies that the *entire* Kerr Penrose diagram depicted above is stable, in particular, spacetime is globally extendible as a C^0 metric across a *bifurcate* null Cauchy horizon such that *all* future inextendible causal geodesics pass into the extension.

The above result is surprising in view of the presence of a well-known *blue-shift instability* [58] associated with the Cauchy horizon, which provided the original evidence for the conjecture of strong cosmic censorship. The theorem is still compatible, however, with the possibility that for generic initial data, the boundary \mathcal{CH}^+ be singular in a weaker sense, specifically, that the metric in particular fails to be H^1_{loc} in any extension of the maximal Cauchy development. (This is related to the Christodoulou formulation of strong cosmic censorship and has been discussed in [14].) Proving this is in turn related to obtaining a suitable *lower* bound on the rate of approach to Kerr on \mathcal{H}^+ in the statement of Conjecture 6.2 for generic initial data. See [21] for further discussion.

Ironically, it is precisely for data lying on the codimension-3 “submanifold” $\mathfrak{M}_{\text{stable}}$ constructed in Theorem 1.1 satisfying $a_{\text{final}} = 0$ for which there is no general analogue of the understanding of the black hole

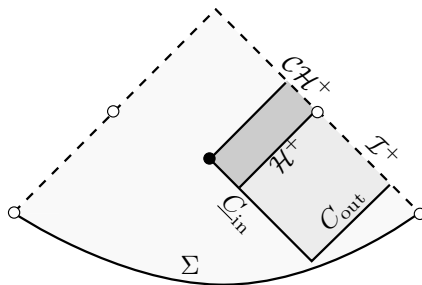


Figure 6: Kerr with $0 < |a| < M$: The Cauchy development of characteristic data superimposed on the Cauchy development of two-ended spacelike data.

interior provided by the above theorem. This case is harder from the perspective of the interior because of the strongly singular nature of the exact Schwarzschild boundary. In the special case of polarised axisymmetry studied in [47], for which in particular $a_{\text{final}} = 0$, this spacelike singular boundary has very recently been shown to be globally stable [3] in a suitable sense. This result relies heavily on the polarised assumption, however, and the precise results proven are not expected to carry over outside of the symmetry class. The most basic question one can ask is whether $a_{\text{final}} = 0$ necessarily means that, in contrast to the $a_{\text{final}} \neq 0$ case, there can never exist a Cauchy horizon emanating from “timelike infinity”. Thus, it would already be interesting to prove simply:

Conjecture 6.5 (Black hole interiors of $\mathfrak{M}_{\text{stable}}$ solutions). *For the initial data of Theorem 5.2, the maximal Cauchy development (\mathcal{M}, g) will necessarily contain a terminal indecomposable past set (TIP) whose intersection with $C_{\text{out}} \cup C_{\text{in}}$ has compact closure.*

For the definition of TIPs, see [30]. Informally, one can view the existence of such a TIP as the existence of a “spacelike piece of singularity”. A positive resolution of the above would in particular show that the set of vacuum initial data leading to a TIP whose intersection with spacelike initial data has compact closure, if not open in moduli space, is at least a set of finite codimension. (In contrast, the largest class of examples produced so far, namely the symmetric solutions of [3] discussed above, as well as previous examples due to [29], produced by a scattering construction, are manifestly of infinite codimension in the moduli space.)

References

- [1] L. Andersson, T. Bäckdahl, P. Blue, and S. Ma. Stability for linearized gravity on the Kerr spacetime. *arXiv:1903.03859, preprint*, 2019.
- [2] Y. Angelopoulos, S. Aretakis, and D. Gajic. Nonlinear scalar perturbations of extremal Reissner-Nordström spacetimes. *Ann. PDE*, 6(2): No. 12, 124, 2020.
- [3] S. Alexakis and G. Fournodavlos. Stable space-like singularity formation for axi-symmetric and polarized near-Schwarzschild black hole interiors. *arXiv:2004.00692, preprint*, 2020.
- [4] S. Aretakis. Horizon instability of extremal black holes. *Adv. Theor. Math. Phys.*, 19(3):507–530, 2015.
- [5] J. M. Bardeen and W. H. Press. Radiation fields in the Schwarzschild background. *J. Math. Phys.*, 14(1):7–19, 1973.
- [6] P. Blue and A. Soffer. The wave equation on the Schwarzschild metric. II: Local decay for the spin 2 Regge Wheeler equation. *J. Math. Phys.*, 46:012502, 2005. [Erratum: arXiv:gr-qc/0608073].

- [7] P. Blue and J. Sterbenz. Uniform decay of local energy and the semi-linear wave equation on Schwarzschild space. *Commun. Math. Phys.*, 268 (2):481–504, 2006.
- [8] H. Bondi, M. G. J. van der Burg, and A. W. K. Metzner. Gravitational waves in general relativity. VII. Waves from axi-symmetric isolated systems. *Proc. Roy. Soc. London Ser. A*, 269:21–52, 1962.
- [9] S. Chandrasekhar. On the equations governing the perturbations of the Schwarzschild black hole. *Proc. Roy. Soc. A*, 343(1634):289–298, 1975.
- [10] Y. Choquet-Bruhat and R. P. Geroch. Global aspects of the Cauchy problem in General Relativity. *Comm. Math. Phys.*, 14:329–335, 1969.
- [11] D. Christodoulou. A mathematical theory of gravitational collapse. *Commun. Math. Phys.*, 109(4):613–647, 1987.
- [12] D. Christodoulou. Nonlinear nature of gravitation and gravitational-wave experiments. *Phys. Rev. Lett.*, 67:1486–1489, Sep 1991.
- [13] D. Christodoulou. On the global initial value problem and the issue of singularities. *Class. Quantum Grav.*, 16:A23–A35, 1999.
- [14] D. Christodoulou. *The formation of black holes in general relativity*. EMS Monographs in Mathematics. European Mathematical Society (EMS), Zürich, 2009.
- [15] D. Christodoulou and S. Klainerman. *The global nonlinear stability of the Minkowski space*, volume 41 of *Princeton Mathematical Series*. Princeton University Press, Princeton, NJ, 1993.
- [16] M. Dafermos and G. Holzegel. On the nonlinear stability of higher dimensional triaxial Bianchi-IX black holes. *Adv. Theor. Math. Phys.*, 10(4):503–523, 2006.
- [17] M. Dafermos, G. Holzegel, and I. Rodnianski. Boundedness and decay for the Teukolsky equation on Kerr spacetimes I: The case $|a| \ll M$. *Ann. PDE*, 5(1):Paper No. 2, 118, 2019.
- [18] M. Dafermos, G. Holzegel, and I. Rodnianski. A scattering theory construction of dynamical vacuum black holes. *arXiv:1306.5364*, preprint, 2013. to appear in *J. Diff. Geom.*
- [19] M. Dafermos, G. Holzegel, and I. Rodnianski. The linear stability of the Schwarzschild solution to gravitational perturbations. *Acta Math.*, 222(1):1–214, 2019.
- [20] M. Dafermos, G. Holzegel, I. Rodnianski, and M. Taylor. The non-linear stability of the Schwarzschild family of black holes. *arXiv:2104.08222*.
- [21] M. Dafermos and J. Luk. The interior of dynamical vacuum black holes I: The C^0 -stability of the Kerr Cauchy horizon. *arXiv:1710.01722*, preprint, 2017.
- [22] M. Dafermos and J. Luk. The interior of dynamical vacuum black holes III: The C^0 -stability of the bifurcation sphere of the Kerr Cauchy horizon. *in preparation*.
- [23] M. Dafermos and I. Rodnianski. A proof of Price’s law for the collapse of self-gravitating scalar field. *Invent. Math.*, 162:381–457, 2005.
- [24] M. Dafermos and I. Rodnianski. The red-shift effect and radiation decay on black hole spacetimes. *Comm. Pure Appl. Math.*, 62:859–919, 2009.
- [25] M. Dafermos and I. Rodnianski. A new physical-space approach to decay for the wave equation with applications to black hole spacetimes. In P. Exner, editor, *XVIIth International Congress on Mathematical Physics*, pages 421–433. World Scientific, London, 2009.

- [26] M. Dafermos and I. Rodnianski. Lectures on black holes and linear waves. In *Evolution equations, Clay Mathematics Proceedings, Vol. 17*, pages 97–205. Amer. Math. Soc., Providence, RI, 2013.
- [27] M. Dafermos, I. Rodnianski, and Y. Shlapentokh-Rothman. Decay for solutions of the wave equation on Kerr exterior spacetimes III: The full subextremal case $|a| < M$. *Ann. of Math. (2)*, 183(3):787–913, 2016.
- [28] Y. Fourès-Bruhat. Théorème d’existence pour certains systèmes d’équations aux dérivées partielles non linéaires. *Acta Math.*, 88:141–225, 1952.
- [29] G. Fournodavlos. On the backward stability of the Schwarzschild black hole singularity. *Commun. Math. Phys.*, 345(3):923–971, 2016.
- [30] R. Geroch, E. H. Kronheimer, and R. Penrose. Ideal points in space-time. *Proc. Roy. Soc. London Ser. A.*, 327(1571):545–567, 1972.
- [31] E. Giorgi. The linear stability of Reissner-Nordström spacetime for small charge. *Ann. PDE*, 6(2):Paper No. 8, 145, 2020.
- [32] E. Giorgi. The linear stability of Reissner-Nordström spacetime: the full subextremal range $|Q| < M$. *Comm. Math. Phys.*, 380(3):1313–1360, 2020.
- [33] E. Giorgi, S. Klainerman, and J. Szeftel. A general formalism for the stability of Kerr. *arXiv:2002.02740, preprint*, 2020.
- [34] D. Häfner, P. Hintz, and A. Vasy. Linear stability of slowly rotating Kerr black holes. *Invent. Math.*, 223(3):1227–1406, 2021.
- [35] P. Hintz and A. Vasy. The global non-linear stability of the Kerr–de Sitter family of black holes. *Acta Math.*, 220(1):1–206, 2018.
- [36] G. Holzegel. Stability and decay rates for the five-dimensional Schwarzschild metric under biaxial perturbations. *Adv. Theor. Math. Phys.*, 14(5):1245–1372, 2010.
- [37] G. Holzegel. General relativity and the analysis of black hole spacetimes. *Lecture notes*, 2022.
- [38] P.-K. Hung. The linear stability of the Schwarzschild spacetime in the harmonic gauge: odd part. *arXiv:1803.03881, preprint*, 2018.
- [39] P.-K. Hung, J. Keller, and M.-T. Wang. Linear stability of Schwarzschild spacetime: decay of metric coefficients. *J. Diff. Geom.*, 116(3):481–541, 2020.
- [40] F. John. Blow-up for quasilinear wave equations in three space dimensions. *Comm. Pure Appl. Math.*, 34(1):29–51, 1981.
- [41] T. W. Johnson. The linear stability of the Schwarzschild solution to gravitational perturbations in the generalised wave gauge. *Ann. PDE*, 5(2):Paper No. 13, 92, 2019.
- [42] R. Kerr. Gravitational field of a spinning mass as an example of algebraically special metrics. *Phys. Rev. Lett.*, 11 (5):237–238, 1963.
- [43] S. Klainerman. Global existence for nonlinear wave equations. *Comm. Pure Appl. Math.*, 33(1):43–101, 1980.
- [44] S. Klainerman. The null condition and global existence to nonlinear wave equations. In *Nonlinear systems of partial differential equations in applied mathematics, Part 1 (Santa Fe, N.M., 1984)*, volume 23 of *Lectures in Appl. Math.*, pages 293–326. Amer. Math. Soc., Providence, RI, 1986.

- [45] S. Klainerman, J. Luk, and I. Rodnianski. A fully anisotropic mechanism for formation of trapped surfaces in vacuum. *Invent. Math.*, 198(1):1–26, 2014.
- [46] S. Klainerman and F. Nicolò. *The evolution problem in general relativity*, volume 25 of *Progress in Mathematical Physics*. Birkhäuser Boston Inc., Boston, MA, 2003.
- [47] S. Klainerman and J. Szeftel. Global nonlinear stability of Schwarzschild spacetime under polarized perturbations. AMS-210. Vol. 395. Princeton University Press, 2020.
- [48] S. Klainerman and J. Szeftel. Constructions of GCM spheres in perturbations of Kerr. *Ann. PDE*, 8:Paper No. 17, 2022.
- [49] S. Klainerman and J. Szeftel. Effective results on uniformization and intrinsic GCM spheres in perturbations of Kerr. *Ann. PDE*, 8:Paper No. 18, 2022.
- [50] S. Klainerman and J. Szeftel. Kerr stability for small angular momentum. *arXiv:2104.11857, preprint*, 2021.
- [51] H. Lindblad and I. Rodnianski. The global stability of Minkowski space-time in harmonic gauge. *Ann. of Math.*, 171(3):1401–1477, 2010.
- [52] J. Luk. Weak null singularities in general relativity. *J. Amer. Math. Soc.*, 31(1):1–63, 2018.
- [53] J. Luk and I. Rodnianski. Nonlinear interaction of impulsive gravitational waves for the vacuum Einstein equations. *Camb. J. Math.*, 5(4):435–570, 2017.
- [54] S. Ma. Uniform energy bound and Morawetz estimate for extreme components of spin fields in the exterior of a slowly rotating Kerr black hole II: Linearized gravity. *Comm. Math. Phys.*, 377(3):2489–2551, 2020.
- [55] C. W. Misner, K. S. Thorne, and J. A. Wheeler. *Gravitation*. Princeton University Press, 2017.
- [56] K. Murata, H. S. Reall, and N. Tanahashi. What happens at the horizon(s) of an extreme black hole? *Classical Quantum Gravity*, 30(23):235007, 36, 2013.
- [57] E. Newman and R. Penrose. An approach to gravitational radiation by a method of spin coefficients. *J. Math. Phys.*, 3(3):566–578, 1962.
- [58] R. Penrose and C. DeWitt. Battelle rencontres. *New York*, page 222, 1968.
- [59] F. Pretorius and W. Israel. Quasispherical light cones of the Kerr geometry. *Class. Quant. Grav.*, 15:2289–2301, 1998.
- [60] T. Regge and J. A. Wheeler. Stability of a Schwarzschild Singularity. *Phys. Rev.*, 108:1063–1069, 1957.
- [61] A. D. Rendall. Reduction of the characteristic initial value problem to the Cauchy problem and its applications to the Einstein equations. *Proc. Roy. Soc. London Ser. A*, 427(1872):221–239, 1990.
- [62] R. Teixeira da Costa and Y. Shlapentokh-Rothman. Boundedness and decay for the Teukolsky equation on Kerr in the full subextremal range $|a| < M$: frequency space analysis. *arXiv:2007.07211, preprint*, 2020.
- [63] R. Sachs. Asymptotic symmetries in gravitational theory. *Phys. Rev.*, 128:2851–2864, Dec 1962.
- [64] J. Sbierski. Characterisation of the energy of Gaussian beams on Lorentzian manifolds: with applications to black hole spacetimes. *Anal. PDE*, 8:1379–1420, 2015.
- [65] S. A. Teukolsky. Perturbations of a rotating black hole. I. Fundamental equations for gravitational, electromagnetic, and neutrino-field perturbations. *Astrophysical J.*, 185:635–648, 1973.

- [66] R. M. Wald. Note on the stability of the Schwarzschild metric. *J. Math. Phys.*, 20:1056–1058, 1979.
- [67] R. M. Wald. *General Relativity*. The University of Chicago Press, Chicago, 1984.